15. Ito, R., I. Katano, K. Kawai, H. Hirata, T. Ogura, T. Kamisako, T. Eto, and M. Ito. 2009. Highly sensitive model for xenogenic GVHD using severe immunodeficient NOG mice. *Transplantation* 87: 1654–1658.
16. van Rijn, R. S., E. R. Simonetti, A. Hagenbeek, M. C. Hogenes, R. A. de Weger, M. R. Canninga-van Dijk, K. Weijer, H. Spits, G. Storm, L. van Bloois, et al. 2003. A new xenograft model for graft-versus-host disease by intravenous transfer of human peripheral blood mononuclear cells in RAG2$^{-/-}$ gammac$^{-/-}$ double-mutant mice. *Blood* 102: 2522–2531.
17. Ito, M., H. Hiramatsu, K. Kobayashi, K. Suzue, M. Kawahata, K. Hioki, Y. Ueyama, Y. Koyanagi, K. Sugamura, K. Tsuji, et al. 2002. NOD/SCID/gamma (c)(null) mouse: an excellent recipient mouse model for engraftment of human cells. *Blood* 100: 3175–3182.
18. Hiramatsu, H., R. Nishikomori, T. Heike, M. Ito, K. Kobayashi, K. Katamura, and T. Nakahata. 2003. Complete reconstitution of human lymphocytes from cord blood CD34+ cells using the NOD/SCID/gammacnull mice model. *Blood* 102: 873–880.
19. Yahata, T., K. Ando, Y. Nakamura, Y. Ueyama, K. Shimamura, N. Tamaoki, S. Kato, and T. Hotta. 2002. Functional human T lymphocyte development from cord blood CD34+ cells in nonobese diabetic/Shi-scid, IL-2 receptor gamma null mice. *J. Immunol.* 169: 204–209.
20. Shultz, L. D., B. L. Lyons, L. M. Burzenski, B. Gott, X. Chen, S. Chaleff, M. Kotb, S. D. Gillies, M. King, J. Mangada, et al. 2005. Human lymphoid and myeloid cell development in NOD/LtSz-scid IL2R gamma null mice engrafted with mobilized human hemopoietic stem cells. *J. Immunol.* 174: 6477–6489.
21. Traggiai, E., L. Chicha, L. Mazzucchelli, L. Bronz, J. C. Piffaretti, A. Lanzavecchia, and M. G. Manz. 2004. Development of a human adaptive immune system in cord blood cell-transplanted mice. *Science* 304: 104–107.
22. Goldman, J. P., M. P. Blundell, L. Lopes, C. Kinnon, J. P. Di Santo, and A. J. Thrasher. 1998. Enhanced human cell engraftment in mice deficient in RAG2 and the common cytokine receptor gamma chain. *Br. J. Haematol.* 103: 335–342.
23. Ito, M., K. Kobayashi, and T. Nakahata. 2008. NOD/Shi-scid IL2rgamma(null) (NOG) mice more appropriate for humanized mouse models. *Curr. Top. Microbiol. Immunol.* 324: 53–76.
24. Manz, M. G. 2007. Human-hemato-lymphoid-system mice: opportunities and challenges. *Immunity* 26: 537–541.
25. Egeland, T., R. Steen, H. Quarsten, G. Gaudernack, Y. C. Yang, and E. Thorsby. 1991. Myeloid differentiation of purified CD34+ cells after stimulation with recombinant human granulocyte-monocyte colony-stimulating factor (CSF), granulocyte-CSF, monocyte-CSF, and interleukin-3. *Blood* 78: 3192–3199.
26. Brugger, W., W. Möcklin, S. Heimfeld, R. J. Berenson, R. Mertelsmann, and L. Kanz. 1993. Ex vivo expansion of enriched peripheral blood CD34+ progenitor cells by stem cell factor, interleukin-1 beta (IL-1 beta), IL-6, IL-3, interferon-gamma, and erythropoietin. *Blood* 81: 2579–2584.
27. Petzer, A. L., P. W. Zandstra, J. M. Piret, and C. J. Eaves. 1996. Differential cytokine effects on primitive (CD34+CD38−) human hematopoietic cells: novel responses to Flt3-ligand and thrombopoietin. *J. Exp. Med.* 183: 2551–2558.
28. Ohmizono, Y., H. Sakabe, T. Kimura, S. Tanimukai, T. Matsumura, H. Miyazaki, S. D. Lyman, and Y. Sonoda. 1997. Thrombopoietin augments ex vivo expansion of human cord blood-derived hematopoietic progenitors in combination with stem cell factor and flt3 ligand. *Leukemia* 11: 524–530.
29. Piacibello, W., L. Fubini, F. Sanavio, M. F. Brizzi, A. Severino, L. Garetto, A. Stacchini, L. Pegoraro, and M. Aglietta. 1995. Effects of human FLT3 ligand on myeloid leukemia cell growth: heterogeneity in response and synergy with other hematopoietic growth factors. *Blood* 86: 4105–4114.
30. Billerbeck, E., W. T. Barry, K. Mu, M. Dorner, C. M. Rice, and A. Ploss. 2011. Development of human CD4+FoxP3+ regulatory T cells in human stem cell factor-, granulocyte-macrophage colony-stimulating factor-, and interleukin-3-expressing NOD-SCID IL2Rγ(null) humanized mice. *Blood* 117: 3076–3086.
31. Rongvaux, A., T. Willinger, H. Takizawa, C. Rathinam, W. Auerbach, A. J. Murphy, D. M. Valenzuela, G. D. Yancopoulos, E. E. Eynon, S. Stevens, et al. 2011. Human thrombopoietin knockin mice efficiently support human hematopoiesis in vivo. *Proc. Natl. Acad. Sci. USA* 108: 2378–2383.
32. Takagi, S., Y. Saito, A. Hijikata, S. Tanaka, T. Watanabe, T. Hasegawa, S. Mochizuki, J. Kunisawa, H. Kiyono, H. Koseki, et al. 2012. Membrane-bound human SCF/KL promotes in vivo human hematopoietic engraftment and myeloid differentiation. *Blood* 119: 2768–2777.
33. Fukuchi, Y., Y. Miyakawa, M. Kizaki, A. Umezawa, K. Shimamura, K. Kobayashi, T. Kuramochi, J. Hata, Y. Ikeda, N. Tamaoki, et al. 1999. Human acute myeloblastic leukemia-ascites model using the human GM-CSF- and IL-3-releasing transgenic SCID mice. *Ann. Hematol.* 78: 223–231.
34. Pawankar, R., M. Okuda, H. Yssel, K. Okumura, and C. Ra. 1997. Nasal mast cells in perennial allergic rhinitics exhibit increased expression of the Fc epsilonRI, CD40L, IL-4, and IL-13, and can induce IgE synthesis in B cells. *J. Clin. Invest.* 99: 1492–1499.
35. Yamaguchi, M., K. Sayama, K. Yano, C. S. Lantz, N. Noben-Trauth, C. Ra, J. J. Costa, and S. J. Galli. 1999. IgE enhances Fc epsilon receptor I expression and IgE-dependent release of histamine and lipid mediators from human umbilical cord blood-derived mast cells: synergistic effect of IL-4 and IgE on human mast cell Fc epsilon receptor I expression and mediator release. *J. Immunol.* 162: 5455–5465.
36. Suemizu, H., C. Yagihashi, T. Mizushima, T. Ogura, T. Etoh, K. Kawai, and M. Ito. 2008. Establishing EGFP congenic mice in a NOD/Shi-scid IL2Rg(null) (NOG) genetic background using a marker-assisted selection protocol (MASP). *Exp. Anim.* 57: 471–477.
37. Knol, E. F., F. P. Mul, H. Jansen, J. Calafat, and D. Roos. 1991. Monitoring human basophil activation via CD63 monoclonal antibody 435. *J. Allergy Clin. Immunol.* 88: 328–338.
38. Irani, A. A., N. M. Schechter, S. S. Craig, G. DeBlois, and L. B. Schwartz. 1986. Two types of human mast cells that have distinct neutral protease compositions. *Proc. Natl. Acad. Sci. USA* 83: 4464–4468.
39. Schafer, B., A. M. Piliponsky, T. Oka, C. H. Song, N. P. Gerard, C. Gerard, M. Tsai, J. Kalesnikoff, and S. J. Galli. 2013. Mast cell anaphylatoxin receptor expression can enhance IgE-dependent skin inflammation in mice. *J. Allergy Clin. Immunol.* 131: 541–548.e1–9.
40. Lynch, D. M., and P. H. Kay. 1995. Studies on the polymorphism of the fifth component of complement in laboratory mice. *Exp. Clin. Immunogenet.* 12: 253–260.
41. Willinger, T., A. Rongvaux, H. Takizawa, G. D. Yancopoulos, D. M. Valenzuela, A. J. Murphy, W. Auerbach, E. E. Eynon, S. Stevens, M. G. Manz, and R. A. Flavell. 2011. Human IL-3/GM-CSF knock-in mice support human alveolar macrophage development and human immune responses in the lung. *Proc. Natl. Acad. Sci. USA* 108: 2390–2395.
42. Zandstra, P. W., E. Conneally, A. L. Petzer, J. M. Piret, and C. J. Eaves. 1997. Cytokine manipulation of primitive human hematopoietic cell self-renewal. *Proc. Natl. Acad. Sci. USA* 94: 4698–4703.
43. Kambe, N., H. Hiramatsu, M. Shimonaka, H. Fujino, R. Nishikomori, T. Heike, M. Ito, K. Kobayashi, Y. Ueyama, N. Matsuyoshi, et al. 2004. Development of both human connective tissue-type and mucosal-type mast cells in mice from hematopoietic stem cells with identical distribution pattern to human body. *Blood* 103: 860–867.
44. Tanaka, S., Y. Saito, J. Kunisawa, Y. Kurashima, T. Wake, N. Suzuki, L. D. Shultz, H. Kiyono, and F. Ishikawa. 2012. Development of mature and functional human myeloid subsets in hematopoietic stem cell-engrafted NOD/SCID/IL2rγKO mice. *J. Immunol.* 188: 6145–6155.
45. Lorentz, A., and S. C. Bischoff. 2001. Regulation of human intestinal mast cells by stem cell factor and IL-4. *Immunol. Rev.* 179: 57–60.
46. Saito, Y., Y. Kametani, K. Hozumi, N. Mochida, K. Ando, M. Ito, T. Nomura, Y. Tokuda, H. Makuuchi, T. Tajima, and S. Habu. 2002. The in vivo development of human T cells from CD34(+) cells in the murine thymic environment. *Int. Immunol.* 14: 1113–1124.
47. Duez, C., A. Tsicopoulos, A. Janin, I. Tillie-Leblond, G. Thyphronitis, P. Marquillies, Q. Hamid, B. Wallaert, A. B. Tonnel, and J. Pestel. 1996. An in vivo model of allergic inflammation: pulmonary human cell infiltrate in allergen-challenged allergic Hu-SCID mice. *Eur. J. Immunol.* 26: 1088–1093.
48. Herz, U., V. A. Botchkarev, R. Paus, and H. Renz. 2004. Increased airway responsiveness, allergy-type-I skin responses and systemic anaphylaxis in a humanized-severe combined immuno-deficiency mouse model. *Clin. Exp. Allergy* 34: 478–487.
49. Weigmann, B., N. Schughart, C. Wiebe, S. Sudowe, H. A. Lehr, H. Jonuleit, L. Vogel, C. Becker, M. F. Neurath, S. Grabbe, et al. 2012. Allergen-induced IgE-dependent gut inflammation in a human PBMC-engrafted murine model of allergy. *J. Allergy Clin. Immunol.* 129: 1126–1135.

Homeostatic Proliferation of Naive CD4$^+$ T Cells in Mesenteric Lymph Nodes Generates Gut-Tropic Th17 Cells

Takeshi Kawabe,* Shu-lan Sun,* Tsuyoshi Fujita,* Satoshi Yamaki,* Atsuko Asao,* Takeshi Takahashi,*,† Takanori So,* and Naoto Ishii*

Homeostatic proliferation of naive T cells in the spleen and cutaneous lymph nodes supplies memory-phenotype T cells. The "systemic" proliferative responses divide distinctly into fast or slow cell division rates. The fast proliferation is critical for generation of effector memory T cells. Because effector memory T cells are abundant in the lamina propria of the intestinal tissue, "gut-specific" homeostatic proliferation of naive T cells may be important for generation of intestinal effector memory T cells. However, such organ-specific homeostatic proliferation of naive T cells has not yet been addressed. In this study, we examined the gut-specific homeostatic proliferation by transferring CFSE-labeled naive CD4$^+$ T cells into sublethally irradiated mice and separately evaluating donor cell division and differentiation in the intestine, mesenteric lymph nodes (MLNs), and other lymphoid organs. We found that the fast-proliferating cell population in the intestine and MLNs had a gut-tropic $\alpha_4\beta_7^+$ Th17 phenotype and that their production was dependent on the presence of commensal bacteria and OX40 costimulation. Mesenteric lymphadenectomy significantly reduced the Th17 cell population in the host intestine. Furthermore, FTY720 treatment induced the accumulation of $\alpha_4\beta_7^+$IL-17A$^+$ fast-dividing cells in MLNs and eliminated donor cells in the intestine, suggesting that MLNs rather than intestinal tissues are essential for generating intestinal Th17 cells. These results reveal that MLNs play a central role in inducing gut-tropic Th17 cells and in maintaining CD4$^+$ T cell homeostasis in the small intestine. *The Journal of Immunology*, **2013, 190: 5788–5798.**

Mature T cells circulate through the peripheral lymphoid and extralymphoid organs, forming peripheral T cell compartments (1). These compartments are homeostatically regulated (2–4) and consist of three groups of T cells that are phenotypically distinguished by surface Ags: naive T (T_N) cells (CD44^{low}CD62L^{high}), central memory T (T_{CM}) cells (CD44^{high}CD62L^{high}), and effector memory T (T_{EM}) cells (CD44^{high}CD62L^{low}) (1, 5, 6). T_N and T_{CM} cells migrate across high endothelial venules into secondary lymphoid tissues such as lymph nodes, Peyer's patches (PPs), and the spleen (1, 6). In contrast, T_{EM} cells preferentially accumulate in extralymphoid organs, notably in the mucosal tissues of the intestine, lungs, and genital surfaces (6–8). Because most pathogens infect mammalian hosts through mucosal surfaces, T_{EM} cells provide a first line of defense against reinfection (6, 9).

*Department of Microbiology and Immunology, Tohoku University Graduate School of Medicine, Sendai 980-8575, Japan; and †Central Institute for Experimental Animals, Kawasaki 210-0821, Japan

Received for publication November 9, 2012. Accepted for publication March 22, 2013.

This work was supported in part by a grant-in-aid for scientific research on priority areas from the Ministry of Education, Science, Sports, and Culture of Japan, a grant-in-aid for scientific research on priority areas from the Japan Society for the Promotion of Science, and grants from the Japan Science and Technology Agency, the Sumitomo Foundation, the Uehara Memorial Foundation, the Novartis Foundation for the Promotion of Science, and the Yakult Bio-Science Foundation.

Address correspondence and reprint requests to Dr. Naoto Ishii, Department of Microbiology and Immunology, Tohoku University Graduate School of Medicine, 2-1 Seiryo-machi, Aoba-ku, Sendai 980-8575, Japan. E-mail address: ishiin@med.tohoku.ac.jp

Abbreviations used in this article: GVHD, graft-versus-host disease; IBD, inflammatory bowel disease; ILN, inguinal lymph node; MLN, mesenteric lymph node; MLX, mesenteric lymphadenectomized; OX40L, OX40 ligand; PP, Peyer's patch; PPX, Peyer's patch–deficient; SFB, segmented filamentous bacteria; T_{CM}, central memory T; T_{EM}, effector memory T; T_N, naive T.

www.jimmunol.org/cgi/doi/10.4049/jimmunol.1203111

In the small intestine, CD4$^+$ T_{EM} cells are primarily found in the lamina propria and CD8$^+$ T_{EM} cells in the epithelium (10). The T cell population in the intestine induces pathogen-specific immunity and inhibits inappropriate responses to self and harmless Ags, ensuring intestinal homeostasis (10, 11). The effector and memory T cells that populate the intestine are reported to be produced in PPs and mesenteric lymph nodes (MLNs) (6, 11, 12). In PPs, M cells in the epithelium transport luminal Ags to the apical side (13), where dendritic cells wait for them (14–16). These dendritic cells prime and activate T_N cells that enter the PP and induce the expression of $\alpha_4\beta_7$, a gut-homing receptor, on the T cells (17). A certain population of these activated T cells moves from the PPs to MLNs through draining lymphatic ducts, then into the bloodstream through the thoracic duct, and finally accumulates in the intestinal mucosa (11, 18). In contrast, lamina propria–derived CD103$^+$ dendritic cells bearing luminal Ags captured in the intestine (19–21) migrate into MLNs (22, 23), where they activate and induce $\alpha_4\beta_7$ expression on T_N cells (24–26). Gut-tropic T cells generated in MLNs collect in the intestine via recirculation (11). However, the distinct roles for PPs and MLNs in generating gut-homing T cells and maintaining intestinal homeostasis have not been clarified.

The CD4$^+$ T cell population in the small intestine includes a significant number of Th17 cells (27). Th17 cells produce the cytokine IL-17A, which is critically involved not only in protecting mucosal tissues from pathogenic infection (28, 29) but also in pathogenesis for immune disorders, such as inflammatory bowel diseases (IBDs) and graft-versus-host disease (GVHD) (30). To understand Th17-mediated immune responses and its disorders, it is important to understand where and how these Th17 cells are generated. Although some types of dendritic cells critically contribute to generating or maintaining the Th17 cell population in the intestine (31), it is not known whether these dendritic cells produce Th17 cells in the lamina propria or whether

T cells in MLNs differentiate into Th17 cells after being primed by migrating dendritic cells.

Homeostatic proliferation is a proliferative T cell response elicited by lymphopenia (2, 4). This systemic proliferative response contributes not only to maintenance of T cell homeostasis (2, 4) but also to pathogenesis for inflammatory diseases including IBDs and GVHD (32–35). The systemic homeostatic proliferation has been studied by transferring T cells into lymphopenic hosts, such as sublethally irradiated or Rag-deficient mice, and examining division and differentiation of donor cells in the spleen and/or cutaneous lymph nodes (36–39). Because the homeostatic proliferation of donor T_N cells supplies a memory–phenotype T cell pool (40–45), this system can be used to determine the origin of intestinal T_{EM} cells, including Th17 cells. It is important to note that in the systemic homeostatic proliferation under lymphopenic conditions, cell populations can be divided into two groups by their division rate—slow, in which cells divide only once or twice per week, and fast, in which cells divide more than seven times within 7 d (46, 47). Slow proliferation depends on IL-7, occurs in secondary lymphoid organs, and produces a cell population that retains the $CD44^{low}CD62L^{high}$ naive phenotype and has limited differentiation potential (2). In contrast, fast proliferation produces cells that robustly differentiate into the $CD44^{high}CD62L^{low}$ T_{EM}–phenotype cells (46, 47). However, it is unclear whether the two distinct types of homeostatic proliferations may also occur in an organ-specific fashion such as in the intestine and MLNs. And if so, the question of where and how fast proliferation occurs, and which organs accumulate the fast-dividing cells, has not yet been resolved.

In this study, we examined the gut-specific homeostatic proliferation in MLNs and intestinal tissue and demonstrated that the fast-dividing population derived from donor $CD4^+$ T_N cells accumulates in the host's small intestine. Fast proliferation occurs in the MLNs dependently of OX40 costimulation and requires the presence of commensal gut flora, which leads to production of gut-tropic T cells. Although PPs affect T cell accumulation in the intestine, they are dispensable for generating $\alpha_4\beta_7^+$ T cells. MLNs, however, play a critical role in priming intestinal Th17 cells. This study identifies MLNs as an essential site of fast homeostatic proliferation and shows that MLNs are essential in regulating Th17 cell homeostasis in the small intestine.

Materials and Methods

Mice

$Ly5.2^+$ C57BL/6 mice between 6 and 8 wk of age were purchased from Japan SLC (Hamamatsu, Japan); $Ly5.1^+$ C57BL/6 mice have been described previously (35). Aly/aly mice were purchased from CLEA Japan (Tokyo, Japan). All mice were maintained under specific pathogen-free conditions at the Institute for Animal Experimentation, Tohoku University Graduate School of Medicine. All procedures were performed according to protocols approved by the Institutional Committee for the Use and Care of Laboratory Animals of Tohoku University.

Generation of PP-deficient mice

PP-deficient (PPX) mice were generated following the protocol described by Nishikawa and colleagues (48). Briefly, 2 mg A7R34, a mAb against the IL-7R α-chain, was administered i.v. to pregnant C57BL/6 mice at 14.5 d postcoitus. Control rat IgG (Life Technologies Japan, Tokyo, Japan) was injected to generate control mice. A7R34 was a gift from S. Nishikawa (Center for Developmental Biology, RIKEN, Kobe, Japan). PP deficiency in the offspring was confirmed by macroscopic inspection of unirradiated mice.

Intestinal surgery

Mesenteric lymphadenectomy was performed following the procedure by Pabst and colleagues (49). In brief, a median incision was made in the abdomen, exposing the MLNs, vessels, and intestine from the end of the duodenum to the colon, and mesenteric lymphadenectomy was performed by microdissection along the length of the superior mesenteric artery to the aortic root. Branch vessels supplying the nodes were cauterized with a Gemini Cautery System (Roboz Surgical Instrument, Gaithersburg, MD), protecting the superior mesenteric artery, vein, and branch vessels supplying the intestine. The abdomen was closed with a 6-0 silk suture (Natsume Seisakusho, Tokyo, Japan). For sham operations, the same procedure was performed without removing the MLNs. These mice were used for each transfer experiment 10 d after the surgery. When these mice were sacrificed, MLN deficiency was confirmed by careful macroscopic inspection.

Antibiotic treatment and 16S rRNA gene quantitative PCR analysis

Mice were treated with ampicillin (1 g/l), neomycin (1 g/l), vancomycin (0.5 g/l), and metronidazole (1 g/l) (Sigma-Aldrich, St. Louis, MO) in drinking water for 3 wk. For the determination of gut microflora, bacterial genomic DNA was isolated from feces using QIAamp DNA Stool Mini Kit (Qiagen, Hilden, Germany), and real-time PCR was done using SYBR Premix Ex Taq (Takara Bio, Otsu, Japan). Quantitative PCR analysis was carried out using a 7500 real-time PCR system (Life Technologies Japan). The real-time PCR program started at an initial step at 95°C for 10 s, followed by 40 cycles of 30 s at 95°C, 30 s at 60°C, and 36 s at 72°C. Data were acquired at the final step at 72°C. Relative quantity was calculated by a ΔCt method and normalized to the amount of *GAPDH*, the amount of which was not affected by antibiotic treatment (data not shown), and presented as relative fold change to an external sample. The following primer sets were used: total bacteria, 5′-GGTGAATACGTTCCCGG-3′ and 5′TACGGCTACCTTGTTACGACTT-3′; *Clostridium leptum*, 5′-CCTTCCGTGCCGSAGTTA-3′ and 5′-GAATTAAACCACATACTCCACTGCTT-3′; segmented filamentous bacteria (SFB), 5′-AGGAGGAGTCTGCGGCACATTAGC-3′ and 5′-CGCATCCTTTACGCCCAGTTATTC-3′; *Bacteroides*, 5′-CCAGCAGCCGCGGTAATA-3′ and 5′-CGCATTCCGCATACTTCTC-3′; and *GAPDH*, 5′-CCAGGTTGTCTCCTGCGACTT-3′ and 5′-CCTGTTGCTGTAGCCGTATTCA-3′.

Adoptive transfer

$CD4^+$ T_N cells ($CD44^{low}CD62L^{high}$) were purified from the spleen of $Ly5.1^+$ C57BL/6 mice by cell sorting using a FACSAria II (BD Biosciences, San Jose, CA). The purity was >99%. $CD4^+$ T_N cells were labeled with CFSE (Life Technologies Japan), and 1.5×10^6 cells were transferred intravenously into $Ly5.2^+$ recipient C57BL/6 mice that had been subjected to sublethal irradiation (5 Gy) 1 d before the transfer. In some experiments, 300 μg blocking anti-OX40 ligand (OX40L) mAb (50) or control rat IgG was injected i.p. into recipient mice every 2 d, beginning 1 d before the transfer. FTY720 (1.0 mg/kg body weight; Cayman Chemical, Ann Arbor, MI) dissolved in PBS, or control PBS alone, was administered i.p. to recipient mice each day, beginning 1 d after the transfer.

Isolation of lymphocytes

Single-cell suspensions were prepared from the spleen, PPs, and peripheral lymph nodes. Lymphocytes from the lamina propria of the small intestine were isolated following the method described by Honda and colleagues (51). Briefly, the small intestine was opened lengthwise, washed to remove fecal content, and cut into small pieces. The pieces were stirred in RPMI 1640 medium containing 2% FCS and 2 mM EDTA for 20 min at 37°C. After epithelial cells and intraepithelial lymphocytes were removed, the tissues were cut into much smaller pieces. These pieces were stirred in RPMI 1640 medium containing 2% FCS, 400 U/ml collagenase type IV, and 0.2 mg/ml DNase I (Sigma-Aldrich) for 20 min at 37°C, twice. Lymphocytes were then purified from the digested tissues by density–gradient centrifugation using Lympholyte M (Cedarlane Labs, Burlington, ON, Canada).

Flow cytometry

Cells from the small intestine, peripheral lymph nodes, spleen, and PPs were prepared and suspended in PBS containing 2% FCS and 0.02% NaN_3. Cells were incubated with a CD16/32 mAb (2.4G2) and stained for 30 min on ice with Abs against cell surface markers. CD4-PE (RM4-5), CD4-Pacific Blue (RM4-5), CD62L-FITC (MEL14), CD44-allophycocyanin (IM7), CD45.1 (Ly5.1)-PE (A20), anti–IFN-γ-allophycocyanin (XMG1.2), anti–IL-17A-BrilliantViolet421 (TC11-18H10.1), anti–CCR9-AlexaFluor647 (CW-1.2), and anti–CCR6-BrilliantViolet421 (29-2L17) were purchased from BioLegend (San Diego, CA). CD44-PE-Cy7 (IM7) and anti-$\alpha_4\beta_7$-allophycocyanin (DATK32) were obtained from eBioscience (San Diego, CA). Anti–OX40-biotin (OX86) was obtained from BD Biosciences. Anti-OX40L

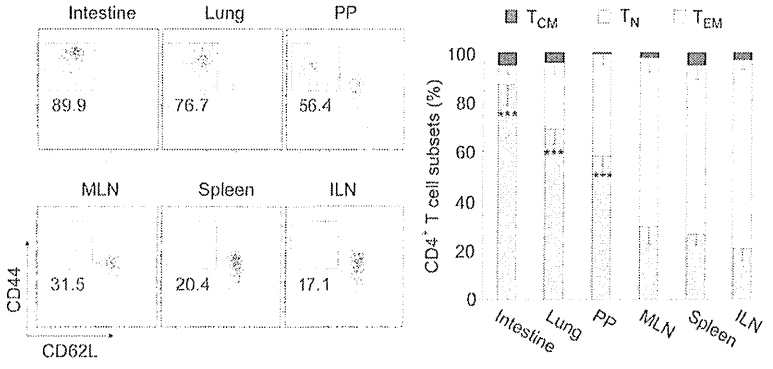

FIGURE 1. The small intestine harbors numerous $CD4^+$ T_{EM} cells in the lamina propria. Lymphocytes were harvested from organs of 10-wk-old unimmunized wild-type mice, and the T_N, T_{CM}, and T_{EM} populations in $CD4^+$ T cells in the indicated organs were determined by flow cytometry. Numbers in the FACS plots show the percent frequency of the T_{EM} population in $CD4^+$ cells for each organ. Representative results are shown for four mice in each group. Bar graph: the percent frequency (mean ± SD) of T_N, T_{CM}, and T_{EM} populations in $CD4^+$ T cells in the indicated organs (n = 4 mice per group). T_{EM} frequency in the spleen was statistically examined by comparison with the frequency in other organs. Similar results were obtained in four independent experiments. $^{***}p < 0.001$.

(MGP34) was as described previously (50). Streptavidin–allophycocyanin (BD Biosciences) was used to visualize biotin-labeled Abs. To detect intracellular IFN-γ and IL-17A, lymphocytes were stimulated with 20 ng/ml PMA and 1 μg/ml ionomycin (Sigma-Aldrich) in the presence of monensin (BD Biosciences) for 5 h. Cells were then stained with surface markers, fixed, permeabilized using a Cytofix/Cytoperm kit (BD Biosciences), and stained with fluorochrome-conjugated anti–IFN-γ and anti–IL-17A mAbs. Flow cytometry was performed with a FACSCanto II (BD Biosciences), and the data were analyzed with FACS Diva (BD Biosciences) and FlowJo (Tree Star, Ashland, OR) software.

Statistical analysis

Statistical analysis was performed by Student t test. The p values <0.05 were considered significant.

Results

The small intestine harbors numerous $CD4^+$ T_{EM} cells under steady-state conditions

T_N and T_{CM} cells are reported to circulate through secondary lymphoid tissues, whereas T_{EM} cells accumulate in extralymphoid organs, including the small intestine (1, 6). To confirm this, we looked for naive and memory $CD4^+$ T cell phenotypes, identified by CD44 and CD62L, in various organs under steady-state conditions. Of the $CD4^+$ T cells found in secondary lymphoid tissues including the spleen, inguinal lymph nodes (ILNs), and MLNs, ~70% had a T_N phenotype and 20–30% had a T_{EM} phenotype (Fig. 1). Only a small proportion of T_{CM} cells were detected in these tissues. In

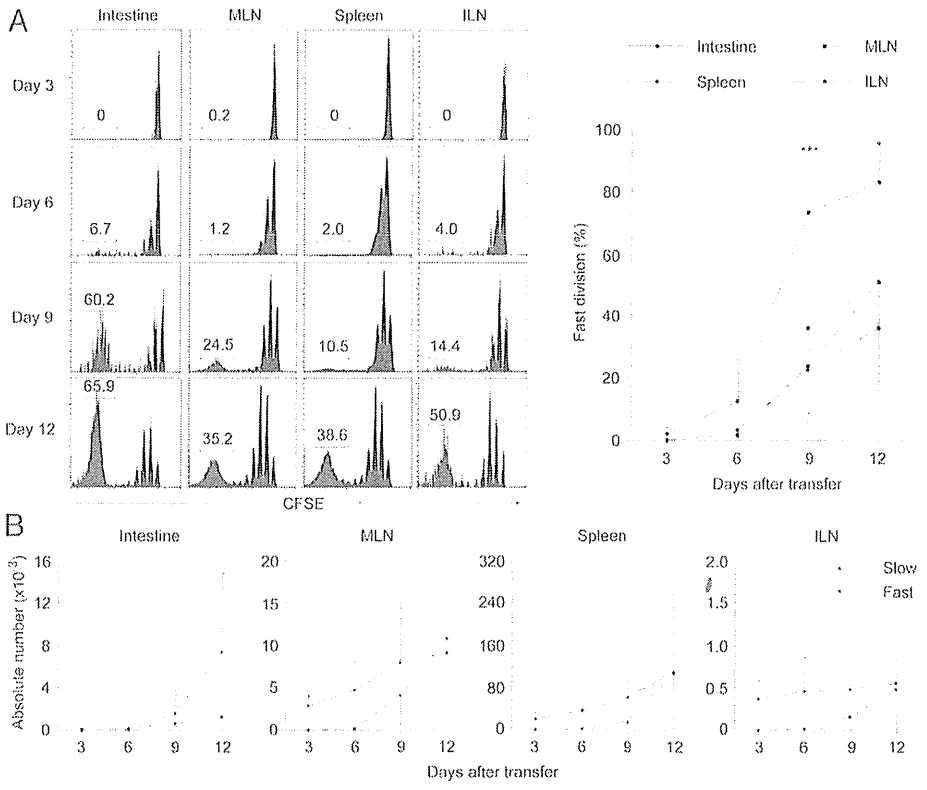

FIGURE 2. Fast-proliferating donor cells preferentially accumulate in the small intestine during homeostatic proliferation. Purified donor $Ly5.1^+CD4^+$ T_N cells were labeled with CFSE and transferred into sublethally irradiated $Ly5.2^+$ recipient mice. CFSE intensity in donor cells from the indicated organs was analyzed on the indicated days after transfer. (**A**) Numbers in FACS panels show the percent frequency of fast-proliferating ($CFSE^-$) cells among the donor cells in each organ. Representative results from five mice are shown. Graph: the percent frequency (mean ± SD) of the fast-proliferating population among donor cells in the indicated organs from five mice on the days indicated. The frequency of the fast-proliferating population among donor cells in the intestine was statistically examined by comparison with the frequency in other organs. (**B**) The number of fast-proliferating (dotted line) and slow-proliferating (solid line) cells (mean ± SD) among donor cells in the indicated organs from five mice on the indicated days. Similar results were obtained in five independent experiments. $^*p < 0.05$, $^{***}p < 0.001$.

PPs, the frequencies of T_N and T_{EM} populations were slightly lower and higher, respectively, than those in the other secondary lymphoid tissues (Fig. 1). By contrast, in the lung and in the lamina propria of the small intestine, >60% of $CD4^+$ T cells had a T_{EM} phenotype (Fig. 1). These data confirm that T_{EM} cells preferentially accumulate in extralymphoid organs, including the small intestine.

Fast-dividing cells accumulate in the small intestine through homeostatic proliferation

Newly generated peripheral $CD4^+$ T cells emerging from the thymus are naive. This suggests that the T_{EM}–phenotype $CD4^+$ T cells found in the small intestine might be activated elsewhere and that the intestine may have a mechanism to preferentially collect and maintain these $CD4^+$ T_{EM} cells. To investigate how T_{EM}–phenotype $CD4^+$ T cells accumulate in the intestine, we organ-specifically examined homeostatic $CD4^+$ T cell proliferation in several lymphoid tissues and the small intestine.

Donor $Ly5.1^+CD4^+$ T_N cells were sorted by FACS, labeled with CFSE, and adoptively transferred into syngeneic $Ly5.2^+$ recipient mice that had been sublethally irradiated. We separately harvested cells from the intestine, MLNs, ILNs, PPs, and the spleen at 3, 6, 9, and 12 d after transfer and analyzed the population and CFSE dilution of donor cells in the respective tissues. Two distinct populations of donor cells even in the intestine and MLNs were distinguished by CFSE dilution—a slow-dividing, $CD62L^{high}$ population with one or two cell division(s) per week, and a fast-dividing, $CD62L^{low}$ population with more than seven cell divisions per week (Fig. 2A; data not shown), as was previously shown in the spleen and/or cutaneous lymph nodes (46, 47). The donor cell population was hardly detected in PPs (data not shown). Both slow- and fast-dividing populations increased during homeostatic proliferation in the intestine, MLNs, ILNs, and the spleen (Fig. 2A, 2B). Slow-dividing cells predominated in lymphoid tissues but were greatly outnumbered by fast-dividing cells in the intestine (Fig. 2A, 2B). These results indicate that fast-proliferating, T_{EM}–phenotype cells preferentially accumulate in the small intestine during homeostatic proliferation.

The fast-dividing cell population in the small intestine depends on PPs and MLNs

We next examined whether the homeostatic proliferation of the donor T cells specifically found in the gut requires lymphoid organs such as PPs and MLNs or whether it occurs in the small intestine itself. We transferred donor T_N cells into irradiated aly/aly mice, in which PPs and peripheral lymph nodes (including MLNs) are defective (52, 53), and monitored the donor cell population in the lamina propria of the small intestine. Although the homeostatic proliferation of donor cells was almost intact in the spleen of aly/aly mice, very few donor T cells could be recovered from the intestine (Fig. 3A, 3B). This suggests that the accumulation of homeostatically proliferating T cells in the small intestine depends on PPs and/or MLNs.

To identify differences in the roles of PPs and MLNs in accumulating donor T cells in the intestine, we generated PPX mice by

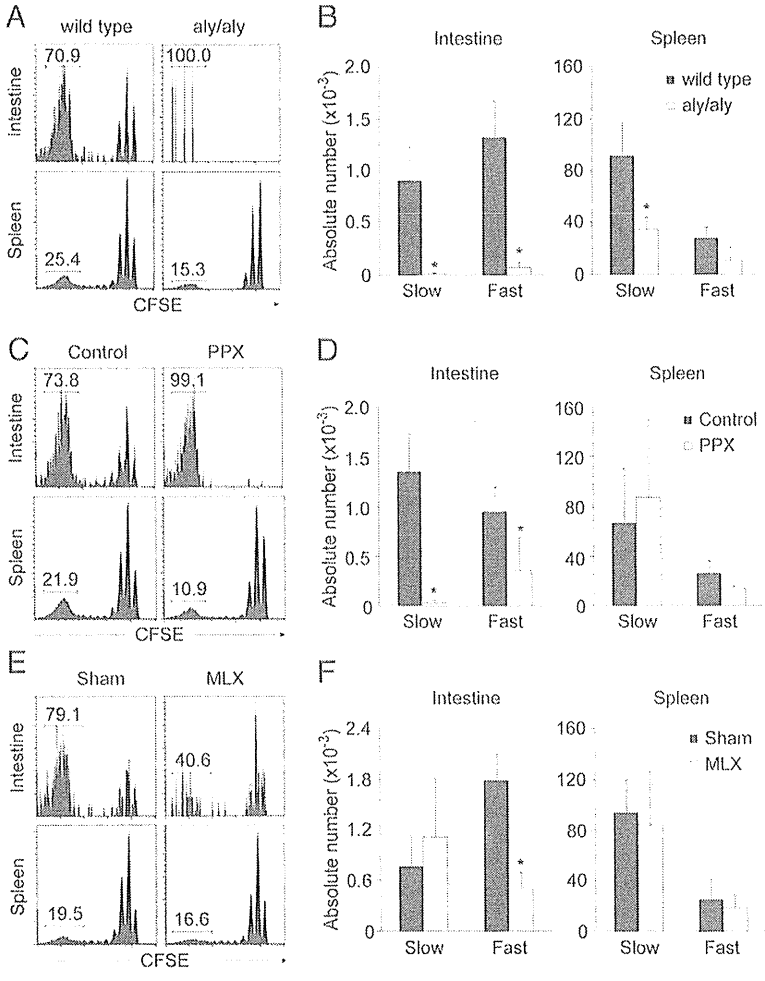

FIGURE 3. Gut-specific homeostatic proliferation of donor T cells requires secondary lymphoid organs. (**A** and **B**) Defective accumulation of donor cells in the intestine of aly/aly mice. Purified CFSE-labeled $Ly5.1^+$ $CD4^+$ T_N cells were transferred into sublethally irradiated $Ly5.2^+$ wild-type (A, *left panel*; B, ■) or aly/aly (A, *right panel*; B, □) mice. CFSE intensity was analyzed in $CD4^+Ly5.1^+$ donor cells harvested from the intestine and the spleen 9 d after the transfer. (A) Numbers in the FACS panels show percent frequency of fast-proliferating populations in $CD4^+Ly5.1^+$ donor cells; representative results for three mice are shown. (B) Absolute numbers (mean ± SD) of fast- and slow-dividing populations in each organ indicated (n = 3 mice/group). Similar results were obtained in three independent experiments. (**C** and **D**) Reduced accumulation of both fast- and slow-dividing donor cells in the intestine of PPX mice. PPX or wild-type (control) recipient mice were used as described in (A) and (B). (C) Numbers in FACS plots show percent frequency of fast-dividing cells among donor cells; results shown are representative of six mice. (D) The number of fast- and slow-proliferating cells (mean ± SD) in each organ (n = 6 mice/group). Similar results were obtained in six independent experiments. (**E** and **F**) Defective accumulation of fast- but not slow-dividing donor cells in the MLX mouse intestine. Recipient MLX or sham-operated (control) mice were used as described in (A) and (B). (E) Numbers in FACS plots show percent frequency of fast-dividing cells among donor cells; results are representative of seven mice. (F) Counts of fast- and slow-proliferating cells (mean ± SD) in each organ indicated (n = 7 mice/group). Similar results were obtained in seven independent experiments. *$p < 0.05$.

injecting a mAb against the IL-7R α-chain into pregnant mice (48). PPs were absent in the offspring at 8 wk of age, but T cell populations in other lymphoid organs were unchanged (data not shown). Slow-dividing donor cells were absent in the small intestine of PPX mice, whereas the fast-dividing population was only marginally smaller than that in control mice (Fig. 3C, 3D). In contrast, donor cell proliferation in the spleen was comparable in PPX and control mice. These results indicate that the slow-dividing population in the small intestine is strongly dependent on PPs, whereas the fast-dividing population is only partly regulated by PPs.

To evaluate the role of MLNs in the homeostatic T cell response in the intestine, donor T_N cells were adoptively transferred into mesenteric lymphadenectomized (MLX) mice in which MLNs had been surgically resected along the superior mesenteric artery to the aortic root. Although the fast-dividing T cell population in the small intestine was significantly smaller in MLX mice than in mice that underwent a sham operation, the slow-dividing population was unchanged (Fig. 3E, 3F). Homeostatic proliferation in the spleen was comparable in MLX and sham-operated mice.

Collectively, these results suggest that the slow-proliferating T cell population in the small intestine depends on PPs but not on MLNs, whereas the fast-proliferating population is mediated by both PPs and MLNs.

MLNs but not PPs are essential for generating gut-homing T cells

The integrin $\alpha_4\beta_7$ and chemokine receptors CCR9 and CCR6 are required for the T cell migration into the intestine (12, 54). We

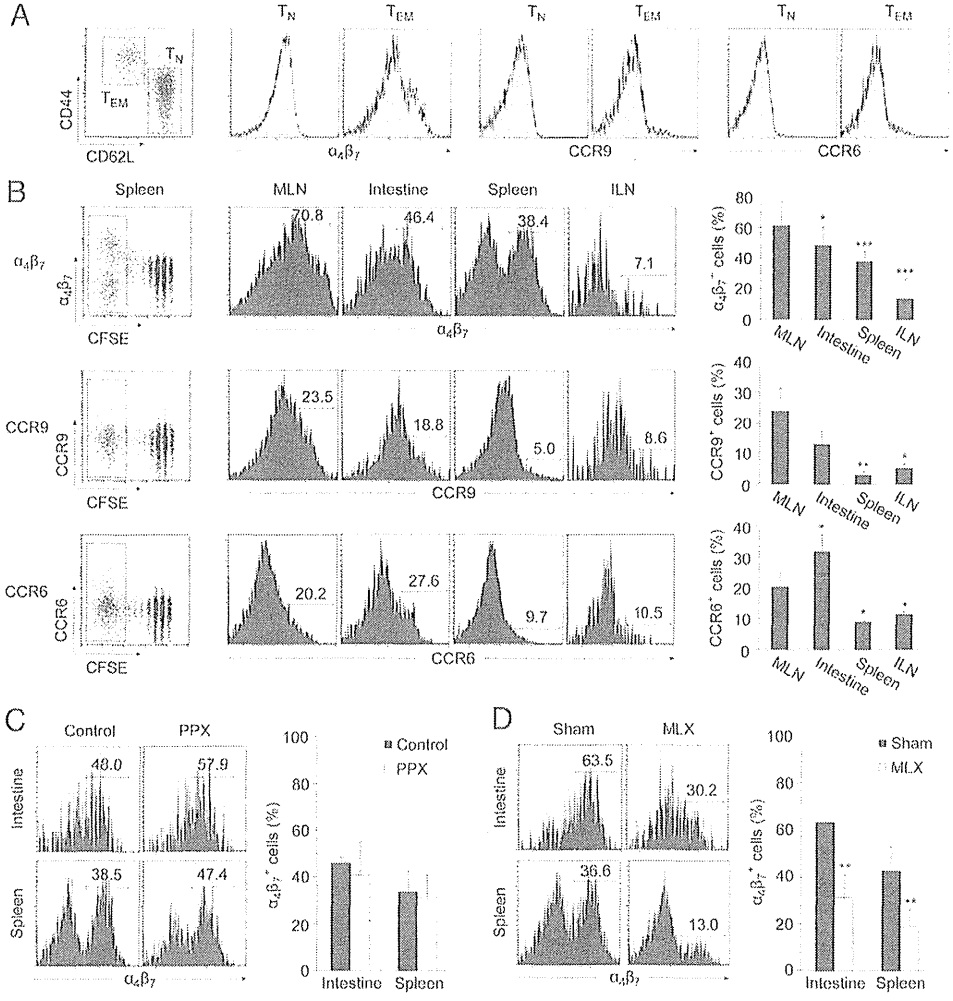

FIGURE 4. Fast homeostatic proliferation generates gut-tropic T cells in MLNs. (**A**) Flow cytometry measurement of $\alpha_4\beta_7$, CCR9, and CCR6 on splenic $CD4^+CD44^{low}CD62L^{high}$ T_N and $CD4^+CD44^{high}CD62L^{low}$ T_{EM} cells in unimmunized wild-type mice under steady-state conditions. Filled histograms: negative control staining. Similar results were obtained in three independent experiments. (**B**) Purified, CFSE-labeled $Ly5.1^+CD4^+$ T_N cells were transferred into sublethally irradiated $Ly5.2^+$ mice, and $\alpha_4\beta_7$ (*top panel*), CCR9 (*middle panel*), and CCR6 (*bottom panel*) expressions on $CD4^+Ly5.1^+CFSE^-$ donor cells in the indicated organs on day 9 were examined by flow cytometry. Numbers in FACS panels show percent frequency of $\alpha_4\beta_7^+$, $CCR9^+$, or $CCR6^+$ cells among fast-proliferating ($CFSE^-$) donor cells. Representative results from three mice are shown. Bar graph: the percent frequency (mean ± SD) of $\alpha_4\beta_7^+$, $CCR9^+$, or $CCR6^+$ cells in $CFSE^-$ donor cells (mean ± SD) from three recipient mice. The frequency of $\alpha_4\beta_7^+$, $CCR9^+$, or $CCR6^+$ cells among $CFSE^-$ donor cells in the indicated organs was statistically examined by comparison with the frequency in MLNs. Similar results were obtained in three independent experiments. (**C** and **D**) MLNs are essential for the optimal generation of $\alpha_4\beta_7^+$ cells. Purified $Ly5.1^+CD4^+$ T_N cells were labeled with CFSE and transferred into sublethally irradiated $Ly5.2^+$ PPX (C) or MLX (D) mice. The $\alpha_4\beta_7^+$ donor cell population in the fast-dividing cells was analyzed as shown in (B). The numbers in FACS panels show the percent frequency of $\alpha_4\beta_7^+$ cells among fast-proliferating ($CFSE^-$) donor cells. Representative results for six mice are shown. Bar graph: the percent frequency (mean ± SD) of $\alpha_4\beta_7^+$ donor cells in $CFSE^-$ donor cells ($n = 6$ mice/group). Similar results were obtained in six independent experiments. $^*p < 0.05$, $^{**}p < 0.01$, $^{***}p < 0.001$.

thus examined $\alpha_4\beta_7$, CCR9, and CCR6 levels on donor cells undergoing homeostatic proliferation. Before transfer, splenic $CD4^+$ T_N cells expressed intermediate levels of $\alpha_4\beta_7$ but undetectable levels of CCR9 and CCR6 (Fig. 4A). After transfer, some donor T cells acquired significant levels of $\alpha_4\beta_7$, CCR9, and CCR6 through fast division (Fig. 4B). In particular, fast-dividing cell populations from the small intestine and MLNs contained larger proportions of the gut-homing receptor-expressing donor cells than did those recovered from the spleen or ILNs (Fig. 4B). In contrast, the slow-dividing populations in these organs retained their initial levels of these receptors (data not shown). These results suggest that the gut-tropic T cells may develop in the small intestine or GALTs during the homeostatic proliferation.

To examine whether PPs and MLNs are required for generating the gut-homing T cells, we determined the frequencies of $\alpha_4\beta_7^+$ donor cells in PPX and MLX mice. The $\alpha_4\beta_7^+$ proportion was unchanged in fast-dividing cells recovered from the small intestine or spleen of PPX mice (Fig. 4C), but the proportion was significantly reduced in MLX mice (Fig. 4D). These findings suggest that MLNs but not PPs are essential for generating $\alpha_4\beta_7^+$ cells through fast cell division.

Donor T cells in the small intestine derive from $\alpha_4\beta_7^+$ cells generated in MLNs via fast proliferation

Having found that MLNs are important for generating fast-proliferating $\alpha_4\beta_7^+$ cells, we postulated that donor $CD4^+$ T_N cells that settle in MLNs rapidly proliferate, acquire the $\alpha_4\beta_7^+$ phenotype, and migrate to the small intestine via recirculation. We tested this by examining homeostatic proliferation in mice treated with the immunomodulatory drug FTY720, which depletes $S1P_1$ on lymphocytes, thus preventing their emigration from secondary lymphoid organs and inducing their accumulation in lymph nodes (55–57). FTY720 treatment significantly increased the number of $\alpha_4\beta_7^+$ cells and decreased the number of $\alpha_4\beta_7^-$ cells in fast-dividing cells recovered from MLNs (Fig. 5A, 5B). In contrast, the number of $\alpha_4\beta_7^+$ cells was markedly reduced in the spleen, whereas the $\alpha_4\beta_7^-$ cell population was unaffected (Fig. 5A, 5B). Therefore, fast proliferation in MLNs may critically contribute to the generation of circulating $\alpha_4\beta_7^+$ cells that are found in the spleen. Furthermore, FTY720 treatment strongly reduced the number of donor cells, including $\alpha_4\beta_7^+$ cells, in the small intestine (Fig. 5C, 5D). These results suggest that $\alpha_4\beta_7^+$ cells may arise from fast-proliferating cells in MLNs and then migrate into the small intestine through recirculation.

Intestinal bacteria promote fast proliferation in MLNs

Fast division during systemic homeostatic proliferation is driven by foreign Ags such as commensal bacteria (46). To determine whether the fast population in MLNs may be induced by commensal bacteria, we examined gut-specific homeostatic proliferation in antibiotic-treated hosts. The removal of commensal bacteria in the hosts' feces by antibiotic treatment was confirmed by quantitative real-time PCR (Fig. 6A). As expected, antibiotic treatment significantly suppressed the generation of fast-proliferating $\alpha_4\beta_7^+$ but not $\alpha_4\beta_7^-$ cells in MLNs (Fig. 6B, 6C). Furthermore, administration of antibiotics strikingly reduced the number of donor cells, including $\alpha_4\beta_7^+$ fast-dividing cells, in the small intestine (Fig. 6D, 6E). Therefore, the commensal microflora is critically involved in the fast proliferation in MLNs.

OX40 signaling is critical for fast proliferation in MLNs

The in vivo blockade of T cell costimulatory signals mediated through OX40, which belongs to the TNF receptor superfamily,

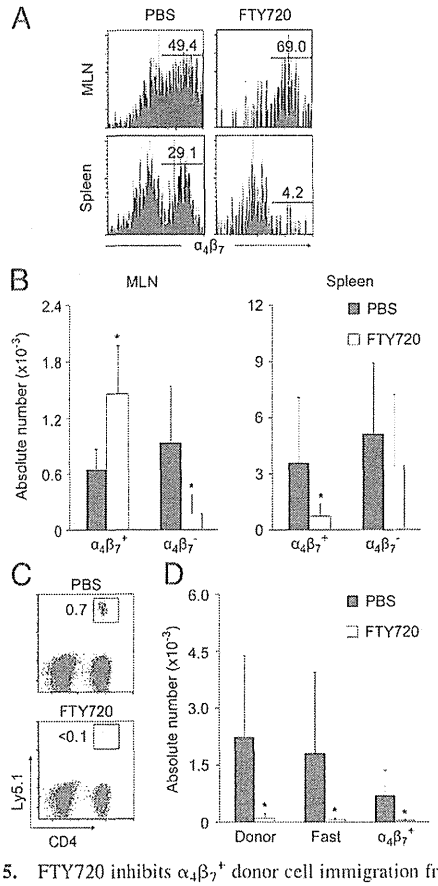

FIGURE 5. FTY720 inhibits $\alpha_4\beta_7^+$ donor cell immigration from MLNs to the small intestine. Purified CFSE-labeled $Ly5.1^+CD4^+$ T_N cells were transferred into sublethally irradiated $Ly5.2^+$ mice treated daily with PBS (■) or FTY720 (□). (**A** and **B**) FTY720 treatment induced $\alpha_4\beta_7^+$ cells to accumulate in MLNs. Levels of $\alpha_4\beta_7$ on fast-proliferating donor cells recovered from MLNs and the spleen 9 d after transfer were evaluated as described in Fig. 4. (A) Numbers in FACS panels show the percent frequency of $\alpha_4\beta_7^+$ cells among $CFSE^-$ donor cells. Representative results are shown for five mice in each group. (B) Graph: the numbers (mean ± SD) of $\alpha_4\beta_7^+$ and $\alpha_4\beta_7^-$ cells in $CFSE^-$ donor cells in each organ (n = 5 mice/group). (**C** and **D**) FTY720 treatment markedly diminished donor cells in the intestine. The donor cell population in the intestine of PBS- or FTY720-treated mice was evaluated by flow cytometry 9 d after transfer. (C) The number in each FACS plot indicates percent frequency of donor cells. Results shown are representative data from five mice in each group. (D) Graph: numbers of total, fast-proliferating, and $\alpha_4\beta_7^+$ donor cells (mean ± SD) in the intestine (n = 5 mice/group). Similar results were obtained in five independent experiments. $^*p < 0.05$.

improves experimental colitis by suppressing the homeostatic proliferation of pathogenic $CD4^+$ T cells (34, 35). Therefore, we examined OX40 expressed on donor T cells in MLNs during homeostatic proliferation and found OX40 on fast- but not slow-proliferating cells (Fig. 7A). To clarify the role of OX40 in fast proliferation, we treated recipient mice with an inhibitory anti-OX40L mAb and monitored donor cell proliferation in MLNs. Treatment with the anti-OX40L mAb significantly inhibited the generation of fast-proliferating $\alpha_4\beta_7^+$ cells in MLNs, without affecting slow cell division (Fig. 7B, 7C). Treatment with the anti-OX40L mAb also strongly reduced the total, fast-proliferating, and $\alpha_4\beta_7^+$ donor T cell populations in the small intestine (Fig. 7D). This indicates that OX40 costimulation is required for generating gut-tropic, fast-dividing cells in MLNs.

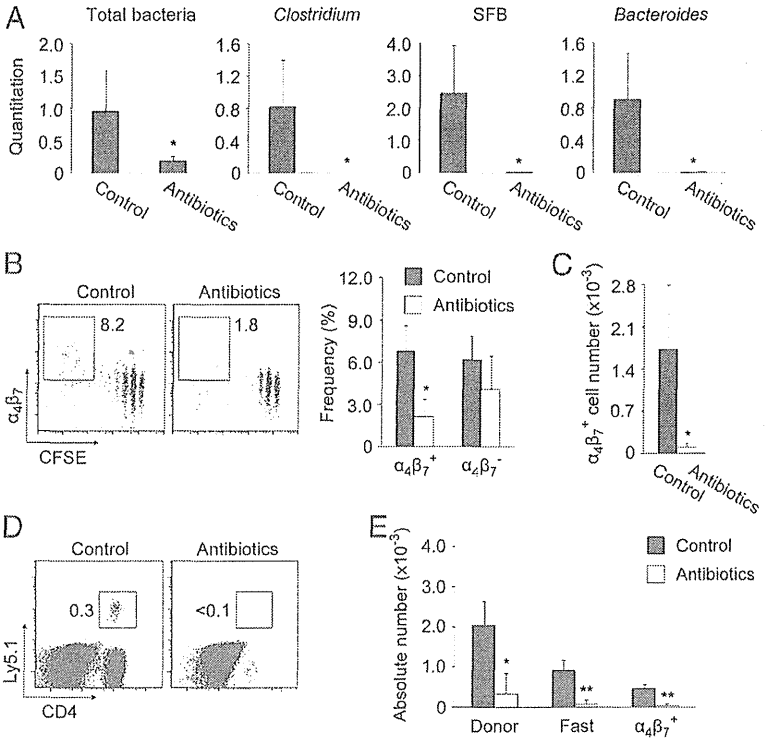

FIGURE 6. Intestinal commensal bacteria are required for fast proliferation in MLNs and the accumulation of donor cells in the intestine. (**A**) Antibiotic treatment deleted commensal gut flora. Bacterial DNA was extracted from feces of antibiotics-treated or non-treated mice, and quantitative PCR analysis for 16s rRNA-coding DNA was carried out. The quantities of total bacteria, *Clostridium*, SFB, and *Bacteroides* (mean ± SD) are indicated (n = 4 mice/group). Similar results were obtained in two independent experiments. (**B–E**) Antibiotics significantly reduced $\alpha_4\beta_7^+$ fast-dividing donor cells in MLNs and diminished donor cells in the intestine. Nine days after adoptive transfer of CFSE-labeled $CD4^+$ T_N cells to antibiotic-treated or control mice, donor cells in MLNs and the intestine were examined by flow cytometry. (B) The number in each FACS panel indicates the percent frequency of $\alpha_4\beta_7^+$ population among donor cells in MLNs. Results shown are representative data of three mice per group. Graph: the percent frequency (mean ± SD) of $\alpha_4\beta_7^+$ or $\alpha_4\beta_7^-$ population among donor cells in MLNs (n = 3 mice/group). (C) Graph: the number (mean ± SD) of $\alpha_4\beta_7^+$ cells among $CFSE^-$ fast-proliferating donor cells in MLNs (n = 3 mice/group). (D) The number in each FACS plot indicates percent frequency of donor cells in the intestine. Results shown are representative data from three mice in each group. (E) Graph: numbers of total, fast proliferating, and $\alpha_4\beta_7^+$ donor cells (mean ± SD) in the intestine (n = 3 mice/group). Similar results were obtained in two independent experiments. $^*p < 0.05$, $^{**}p < 0.01$.

Gut-tropic Th17 cells arise in MLNs during homeostatic proliferation

The $CD4^+$ T cell population in the small intestine includes a significant number of Th17 cells (27). Therefore, we measured IFN-γ and IL-17A cytokine levels in donor cells recovered from the small intestine, spleen, and MLNs. Neither cytokine was produced by the slow-dividing population, whereas the fast-dividing population expressed both (Fig. 8A; data not shown). When gating on the fast-dividing population, an IFN-γ profile was dominant in the spleen (Fig. 8A, spleen), but in the intestine, IL-17A–producing cells greatly outnumbered IFN-γ-producing ones (Fig. 8A, intestine). In MLNs, IFN-γ and IL-17A were detected at equal levels (Fig. 8A, MLN). These results indicate that Th17 cells are generated through fast proliferation in an organ-specific manner and that gut-specific Th17 cells may arise in MLNs or the small intestine.

FTY720 treatment caused $\alpha_4\beta_7^+$ cells to accumulate in MLNs and strongly depleted donor cells in the intestine (Fig. 5). Therefore, if fast homeostatic proliferation in MLNs is responsible for the differentiation of gut-associated Th17 cells, FTY720 treatment should induce donor Th17 cells to accumulate in MLNs. As expected, FTY720 treatment increased the $IL\text{-}17A^+$ population and decreased the $IFN\text{-}\gamma^+$ population in MLNs (Fig. 8B, MLN). However, FTY720 increased the $IFN\text{-}\gamma^+$ population but did not affect the minor $IL\text{-}17A^+$ population found in the spleen (Fig. 8B, spleen). These results suggest that $CD4^+$ T cells that produce IL-17A are almost exclusively generated by MLNs and those producing IFN-γ by the spleen. This result is supported by our finding that MLN-derived $\alpha_4\beta_7^+$ and spleen-derived $\alpha_4\beta_7^-$ populations included $IL\text{-}17A^+$ and $IFN\text{-}\gamma^+$ cells, respectively (data not shown). Furthermore, removing MLNs from recipient mice significantly reduced the $IL\text{-}17A^+$ but not the $IFN\text{-}\gamma^+$ population in the small intestine (Fig. 8C). Collectively, these results demonstrate that MLNs are essential for the generation of gut-tropic Th17 cells through fast homeostatic proliferation.

Discussion

In this study, we examined the homeostatic proliferation of $CD4^+$ T_N cells in an organ-specific manner and found that the two distinct types of homeostatic proliferation, fast and slow, which were discovered in the spleen and cutaneous lymph nodes (46, 47), also occur in MLNs and intestinal tissue. Furthermore, we demonstrated that the fast homeostatic proliferation of $CD4^+$ T_N cells in MLNs critically contributes to the generation of gut-homing T_{EM}–phenotype Th17 cells, indicating an important role of the fast gut-specific proliferation. $CD4^+$ T_{EM} cells, including Th17 cells, represent a significant portion of the intestinal T cell population (27), and control bacterial infections in the gut (28, 29). Therefore, the present results may further our understanding of gut-homing T_{EM} cell differentiation in vivo.

Homeostatic proliferation is a physiological proliferative T cell response induced by an emergent immunological status such as lymphopenia (2). For example, in elderly people, patients thymectomized during early childhood, or patients infected with HIV-1, who are all situated under lymphopenic conditions, homeostatic proliferation contributes to maintaining the T cell number (58). Besides, neonatal mice, which do not yet have sufficient T cells, show the homeostatic proliferation to increase the T cell number up to the physiological status (59, 60). Although we induced lymphopenia by irradiation, the gut-specific homeostatic proliferation may contribute to generation of intestinal Th17 cells under a certain physiological condition.

Several studies have reported that slow homeostatic proliferation is mediated by self peptides/MHC and IL-7 in secondary lymphoid organs (2, 46, 47). Consistent with these studies, we found the slowly proliferating population to be present mainly in secondary lymphoid organs, including the spleen, MLNs, and ILNs (Fig. 2).

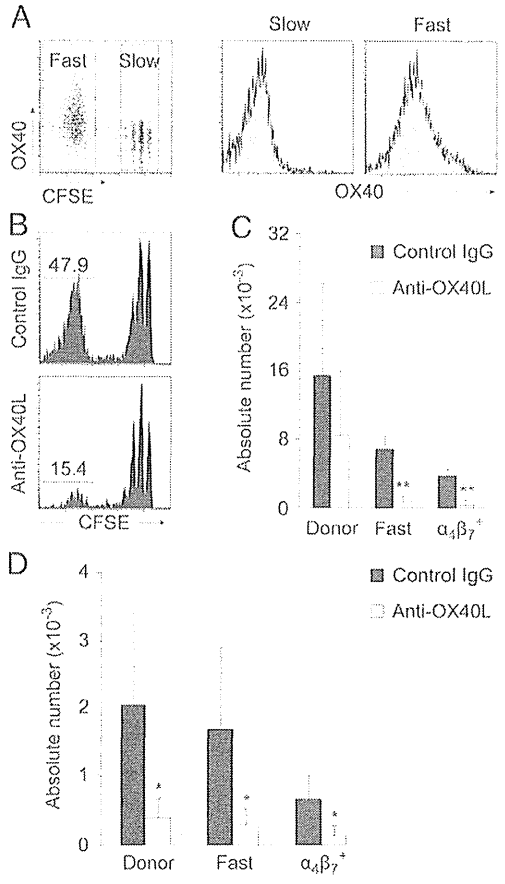

FIGURE 7. Blockade of OX40L–OX40 interactions inhibits fast proliferation in MLNs and the accumulation of donor cells in the small intestine. (**A**) Nine days after adoptive transfer of CFSE-labeled $CD4^+$ T_N cells, OX40 expression on the fast ($CFSE^-$) and slow ($CFSE^{high}$) populations in donor cells in MLNs was examined by flow cytometry. Filled histograms show negative control staining. Similar results were obtained in two independent experiments. (**B–D**) Recipient mice were treated with blocking anti-OX40L mAb or with control rat IgG. Donor cells in MLNs and the intestine were examined by flow cytometry 9 d after transfer. (B) The number in each FACS panel indicates the percent frequency of fast-proliferating cells among donor cells in MLNs. Results shown are representative data of six mice per group. (C) Graph: the number (mean ± SD) of fast-proliferating cells among donor cells in MLNs (n = 6 mice/group). (D) Graph: the numbers of total, fast proliferating, and $\alpha_4\beta_7^+$ donor cells (mean ± SD) in the intestine (n = 6 mice/group). Similar results were obtained in six independent experiments. $^*p < 0.05$, $^{**}p < 0.01$.

However, less has been known about where fast proliferation occurs. Our results show that the $\alpha_4\beta_7^+$ fast-proliferating population is generated mainly in MLNs and that it may contribute to gut-tropic Th17 generation. The organ-specific proliferation may contribute to generation of organ-specific T_{EM} cells.

To our knowledge, this study reveals for the first time that, in addition to commensal bacteria, OX40 costimulation is crucial for inducing fast proliferation. In particular, both commensal bacteria and OX40 are required for fast proliferation in MLNs and for gut-tropic T cell accumulation in the lamina propria of the intestine. Studies in several animal models have demonstrated that OX40–OX40L interactions mediate the development of IBDs and GVHD, both of which are pathogenically associated with the homeostatic proliferation of $CD4^+$ T_N cells (34, 35, 61). Therefore, it is likely that $\alpha_4\beta_7^+$ Th17 cells generated through fast homeostatic proliferation in MLNs are also involved in the pathogenesis of these diseases in an OX40-dependent manner. This possibility led us to examine the OX40L expression on several types of $CD11c^+$MHC II^+ dendritic cells, which may probably present Ags of intestinal commensal bacteria to T cells, in the MLNs of recipient mice, because OX40L is thought to be expressed on APCs such as dendritic cells and B cells (62–64). Because blockading OX40L significantly reduced the number of $\alpha_4\beta_7^+$ cells in the MLNs (Fig. 7C), we speculated that $CD103^+$ dendritic cells, which are important for inducing $\alpha_4\beta_7^+$ T cells (26), might express OX40L. Unexpectedly, we did not find OX40L-expressing dendritic cells in the MLNs of recipient mice, even when the mice were subjected to sublethal irradiation (data not shown). Therefore, a cell population other than $CD11c^+$ dendritic cells may express OX40L and mediate fast proliferation in MLNs. The precise role of OX40 signaling in inducing gut-homing Th17 cells requires further study.

Several studies have demonstrated that MLNs and PPs are important for generating gut-tropic T cells, which express specific markers such as $\alpha_4\beta_7$, CCR9, and CCR6 (12, 54). Previous studies showed that MLN-derived T lymphoblasts preferentially accumulate in the intestine (65, 66). A recent study using a T cell transfer method revealed that donor T cells acquire $\alpha_4\beta_7$ in the MLNs upon in vivo Ag stimulation (24). Other reports found that dendritic cells from MLNs and PPs are capable of inducing $\alpha_4\beta_7^+$ T cells in vitro (17, 25, 67, 68). However, a study using a virus-specific TCR-transgenic T cell system showed that a sufficient number of $\alpha_4\beta_7^+$ T cells were generated in the spleen in response to viral infection, even in mice treated with FTY720, suggesting that MLNs and PPs are dispensable (69). Despite the controversy on the roles of MLNs and PPs, our present study clearly shows that MLNs, but not the spleen or PPs, are essential for generating gut-tropic $\alpha_4\beta_7^+$ effector T cells, because $\alpha_4\beta_7^+$ donor cells in the intestine were markedly reduced in MLN-deficient PP-intact MLX mice (Figs. 3E, 3F, 4D), and a fast-proliferating population was found in the intestine even in MLN-intact PP-deficient PPX mice—but not in MLN-deficient PP-deficient aly/aly mice (Fig. 3A–D). Indeed, the donor cell number in PPs was less than 1/50th of that in MLNs 9 d after transfer (data not shown). Therefore, MLNs, but not PPs, may be the main place for gut-tropic T cell proliferation in our model, although the presence of PPs crucially contributed to distribution of slow proliferating donor cells in the intestine (Fig. 3C, 3D). Furthermore, FTY720 treatment induced $\alpha_4\beta_7^+$ donor cells to accumulate in MLNs, consequently depleting them in the intestine and spleen (Fig. 5); this finding also suggests that MLNs are critical for inducing gut-homing T cells. It is still unclear, however, whether Ag stimulation is required for the homeostatic proliferation-induced generation of gut-tropic T cells despite the indispensability of intestinal flora. The contribution of MLNs to the generation of gut-homing T cells may differ in the context of homeostatic proliferation or Ag-specific activation.

The generation of Th17 cells has been thought to occur in the lamina propria of the intestine (31) in part because the frequency of these cells is much higher in the intestinal lamina propria than in PPs or MLNs (70, 71). Indeed, the lamina propria of the colon is rich in $CX3CR1^+CD103^-CD70^{high}CD11c^{low}$ cells, which have the capacity to generate Th17 cells in vitro (70). It was also recently reported that $CD11c^+$E-cadherin$^+$ cells in the colonic lamina propria and in inflamed MLNs promote Th17 differentiation in vivo (72). However, it is unlikely that the donor T_N cells directly entered the lamina propria of the intestine to be primed for Th17 differentiation by intestinal APCs in our experimental settings, because donor T cells were not found in the intestinal lamina propria of aly/aly mice (Fig. 3A, 3B), and because FTY720

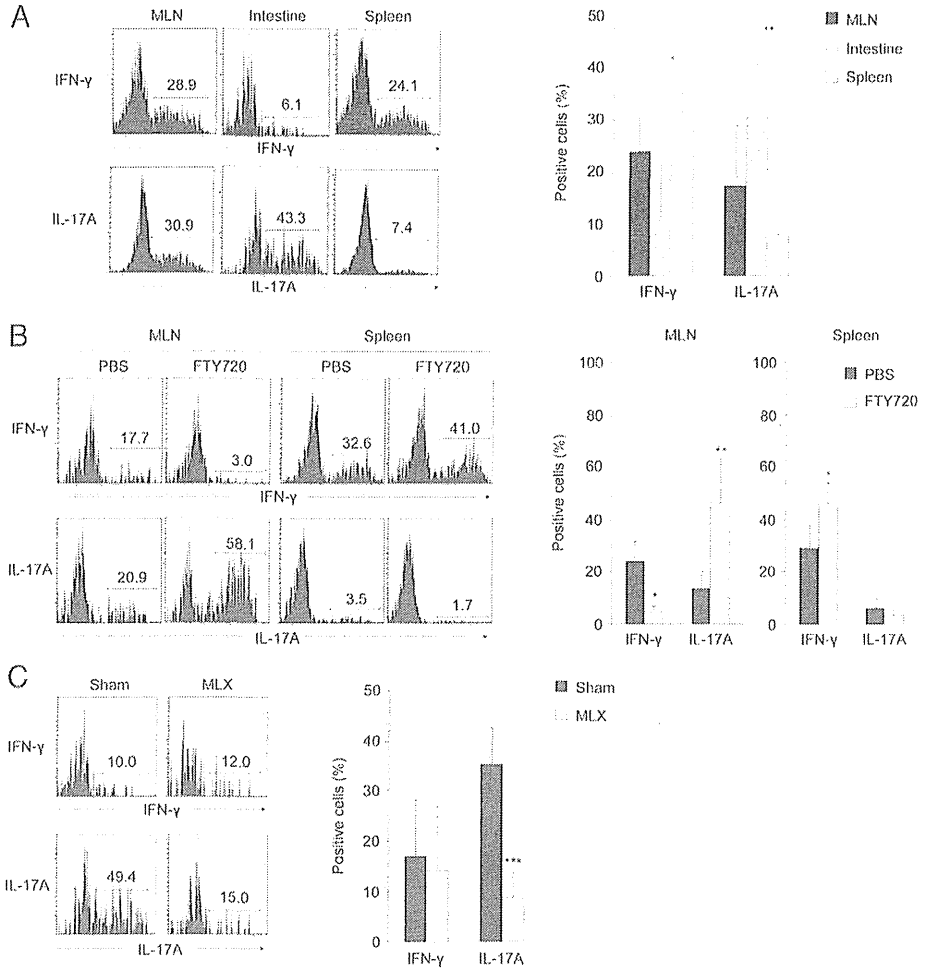

FIGURE 8. Gut-tropic IL-17A$^+$ donor cells arise during fast homeostatic proliferation in MLNs. Nine days after transfer, donor cells were collected from the indicated organs of recipient mice and were stimulated ex vivo with PMA and ionomycin. Intracellular expression of IFN-γ and IL-17A in fast-proliferating donor cell populations was examined by flow cytometry. (**A**) Frequency of IFN-γ– or IL-17A–producing cells among fast-proliferating donor cells in each of the indicated organs. Graph: the mean ± SD from five mice per group. Similar results were obtained in five independent experiments. (**B**) FTY720 treatment, as described in Fig. 5; FACS results shown (*left panel*) are representative of three mice per group. Numbers in FACS histograms indicate percent frequency of IFN-γ– or IL-17A–producing cells among the fast proliferating donor cells in each organ. Graph (*right panel*): the percent frequency of IFN-γ– or IL-17A–producing cells (mean ± SD) among fast-proliferating donor cells in each organ (n = 3 mice/group). Similar results were obtained in two independent experiments. (**C**) MLX or sham-operated control recipient mice. Numbers in FACS histograms indicate percent frequency of cells producing IFN-γ or IL-17A among the fast proliferating donor cells in the lamina propria of the small intestine. Results shown are representative of five mice per group. Graph (*right panel*) represents the percent frequency (mean ± SD) of IFN-γ– or IL-17A–producing cells among fast-proliferating donor cells in the intestinal lamina propria (n = 5 mice/group). Similar results were obtained in five independent experiments. $^*p < 0.05$, $^{**}p < 0.01$, $^{***}p < 0.001$.

treatment or mesenteric lymphadenectomy depleted donor T cells, including Th17 cells, from the intestine (Figs. 5C, 5D, 8C). Th17 cells may be generated in MLNs, after which they may migrate and accumulate in the lamina propria of the small intestine.

Intestinal Th17 cells are induced by SFB, an intestinal commensal bacterium (27). Consistently, the gut-tropic $\alpha_4\beta_7^+$ population, which were rich in Th17 cells (data not shown), was markedly reduced by antibiotic treatment that removed almost all commensal bacteria including SFB (Fig. 6A–C). Therefore, gut-homing Th17 cells are generated dependently of commensal bacteria. By contrast, mechanisms for generating Th1 cells, which were at least in part generated in the spleen (Fig. 8B), are unclear. Because the $\alpha_4\beta_7^-$ fast population, which was rich in the Th1 cells (data not shown), was not affected by antibiotic treatment (Fig. 6B), the Th1 cells may be induced by a different mechanism from Th17 cells, which require intestinal commensal bacteria. Further studies on the distinct mechanisms between Th1 and Th17 generations will be needed.

In summary, our results clearly demonstrate that gut-specific fast homeostatic proliferation plays a critical role in inducing gut-homing $\alpha_4\beta_7^+$IL-17A$^+$ T cells, which is dependent on OX40 signals. Although the systemic inhibition of OX40 signals, either in OX40L-knockout mice or by treatment with an anti-OX40L mAb, drastically ameliorates several types of IBDs and GVHD (34, 35, 61), our study revealed that the OX40–OX40L interactions necessary for generating intestinal Th17 cells may occur in the MLNs. Therefore, it may be possible to develop therapeutic strategies for IBDs and GVHD by controlling the OX40–OX40L interactions in MLNs. In addition, the finding that the role of MLNs in developing gut-homing T_{EM} cells, including Th17 cells, is distinct from that of the PPs or spleen may contribute to a deeper understanding of intestinal mucosal immunity.

Acknowledgments

We thank Dr. S. Nishikawa (RIKEN Center for Developmental Biology, Kobe) for providing A7R34 mAb, Dr. K. Honda (RIKEN Research Center for Allergy and Immunology, Yokohama, Japan), Dr. H. Kudo (Tohoku University, Sendai, Japan), and Dr. J. Komura (Tohoku University) for critical help on experiments, and E. Saijo, H. Abe, and T. Yamashita for assistance. We thank the Biomedical Research Core and the Institute for Animal Experimentation (Tohoku University Graduate School of Medicine) for technical support.

Disclosures

The authors have no conflicting financial interests.

References

1. Butcher, E. C., and L. J. Picker. 1996. Lymphocyte homing and homeostasis. *Science* 272: 60–66.
2. Surh, C. D., and J. Sprent. 2008. Homeostasis of naive and memory T cells. *Immunity* 29: 848–862.
3. Takada, K., and S. C. Jameson. 2009. Naive T cell homeostasis: from awareness of space to a sense of place. *Nat. Rev. Immunol.* 9: 823–832.
4. Sprent, J., and C. D. Surh. 2011. Normal T cell homeostasis: the conversion of naive cells into memory-phenotype cells. *Nat. Immunol.* 12: 478–484.
5. Sallusto, F., D. Lenig, R. Förster, M. Lipp, and A. Lanzavecchia. 1999. Two subsets of memory T lymphocytes with distinct homing potentials and effector functions. *Nature* 401: 708–712.
6. Sheridan, B. S., and L. Lefrançois. 2011. Regional and mucosal memory T cells. *Nat. Immunol.* 12: 485–491.
7. Masopust, D., V. Vezys, A. L. Marzo, and L. Lefrançois. 2001. Preferential localization of effector memory cells in nonlymphoid tissue. *Science* 291: 2413–2417.
8. Reinhardt, R. L., A. Khoruts, R. Merica, T. Zell, and M. K. Jenkins. 2001. Visualizing the generation of memory CD4 T cells in the whole body. *Nature* 410: 101–105.
9. Sallusto, F., A. Lanzavecchia, K. Araki, and R. Ahmed. 2010. From vaccines to memory and back. *Immunity* 33: 451–463.
10. Macdonald, T. T., and G. Monteleone. 2005. Immunity, inflammation, and allergy in the gut. *Science* 307: 1920–1925.
11. Mowat, A. M. 2003. Anatomical basis of tolerance and immunity to intestinal antigens. *Nat. Rev. Immunol.* 3: 331–341.
12. Johansson-Lindbom, B., and W. W. Agace. 2007. Generation of gut-homing T cells and their localization to the small intestinal mucosa. *Immunol. Rev.* 215: 226–242.
13. Neutra, M. R., A. Frey, and J. P. Kraehenbuhl. 1996. Epithelial M cells: gateways for mucosal infection and immunization. *Cell* 86: 345–348.
14. Hopkins, S. A., F. Niedergang, I. E. Corthesy-Theulaz, and J. P. Kraehenbuhl. 2000. A recombinant *Salmonella typhimurium* vaccine strain is taken up and survives within murine Peyer's patch dendritic cells. *Cell. Microbiol.* 2: 59–68.
15. Kunkel, D., D. Kirchhoff, S. Nishikawa, A. Radbruch, and A. Scheffold. 2003. Visualization of peptide presentation following oral application of antigen in normal and Peyer's patches-deficient mice. *Eur. J. Immunol.* 33: 1292–1301.
16. Fleeton, M. N., N. Contractor, F. Leon, J. D. Wetzel, T. S. Dermody, and B. L. Kelsall. 2004. Peyer's patch dendritic cells process viral antigen from apoptotic epithelial cells in the intestine of reovirus-infected mice. *J. Exp. Med.* 200: 235–245.
17. Mora, J. R., M. R. Bono, N. Manjunath, W. Weninger, L. L. Cavanagh, M. Rosemblatt, and U. H. Von Andrian. 2003. Selective imprinting of gut-homing T cells by Peyer's patch dendritic cells. *Nature* 424: 88–93.
18. Guy-Grand, D., C. Griscelli, and P. Vassalli. 1978. The mouse gut T lymphocyte, a novel type of T cell: nature, origin, and traffic in mice in normal and graft-versus-host conditions. *J. Exp. Med.* 148: 1661–1677.
19. Rescigno, M., M. Urbano, B. Valzasina, M. Francolini, G. Rotta, R. Bonasio, F. Granucci, J. P. Kraehenbuhl, and P. Ricciardi-Castagnoli. 2001. Dendritic cells express tight junction proteins and penetrate gut epithelial monolayers to sample bacteria. *Nat. Immunol.* 2: 361–367.
20. Chieppa, M., M. Rescigno, A. Y. Huang, and R. N. Germain. 2006. Dynamic imaging of dendritic cell extension into the small bowel lumen in response to epithelial cell TLR engagement. *J. Exp. Med.* 203: 2841–2852.
21. McDole, J. R., L. W. Wheeler, K. G. McDonald, B. Wang, V. Konjufca, K. A. Knoop, R. D. Newberry, and M. J. Miller. 2012. Goblet cells deliver luminal antigen to CD103$^+$ dendritic cells in the small intestine. *Nature* 483: 345–349.
22. Liu, L. M., and G. G. MacPherson. 1991. Lymph-borne (veiled) dendritic cells can acquire and present intestinally administered antigens. *Immunology* 73: 281–286.
23. Schulz, O., E. Jaensson, E. K. Persson, X. Liu, T. Worbs, W. W. Agace, and O. Pabst. 2009. Intestinal CD103$^+$, but not CX3CR1$^+$, antigen sampling cells migrate in lymph and serve classical dendritic cell functions. *J. Exp. Med.* 206: 3101–3114.
24. Campbell, D. J., and E. C. Butcher. 2002. Rapid acquisition of tissue-specific homing phenotypes by CD4$^+$ T cells activated in cutaneous or mucosal lymphoid tissues. *J. Exp. Med.* 195: 135–141.
25. Johansson-Lindbom, B., M. Svensson, M. A. Wurbel, B. Malissen, G. Márquez, and W. Agace. 2003. Selective generation of gut tropic T cells in gut-associated lymphoid tissue (GALT): requirement for GALT dendritic cells and adjuvant. *J. Exp. Med.* 198: 963–969.
26. Johansson-Lindbom, B., M. Svensson, O. Pabst, C. Palmqvist, G. Marquez, R. Förster, and W. W. Agace. 2005. Functional specialization of gut CD103$^+$ dendritic cells in the regulation of tissue-selective T cell homing. *J. Exp. Med.* 202: 1063–1073.
27. Ivanov, I. I., K. Atarashi, N. Manel, E. L. Brodie, T. Shima, U. Karaoz, D. Wei, K. C. Goldfarb, C. A. Santee, S. V. Lynch, et al. 2009. Induction of intestinal Th17 cells by segmented filamentous bacteria. *Cell* 139: 485–498.
28. Conti, H. R., F. Shen, N. Nayyar, E. Stocum, J. N. Sun, M. J. Lindemann, A. W. Ho, J. H. Hai, J. J. Yu, J. W. Jung, et al. 2009. Th17 cells and IL-17 receptor signaling are essential for mucosal host defense against oral candidiasis. *J. Exp. Med.* 206: 299–311.
29. Ishigame, H., S. Kakuta, T. Nagai, M. Kadoki, A. Nambu, Y. Komiyama, N. Fujikado, Y. Tanahashi, A. Akitsu, H. Kotaki, et al. 2009. Differential roles of interleukin-17A and -17F in host defense against mucoepithelial bacterial infection and allergic responses. *Immunity* 30: 108–119.
30. Kappel, L. W., G. L. Goldberg, C. G. King, D. Y. Suh, O. M. Smith, C. Ligh, A. M. Holland, J. Grubin, N. M. Mark, C. Liu, et al. 2009. IL-17 contributes to CD4-mediated graft-versus-host disease. *Blood* 113: 945–952.
31. Honda, K., and D. R. Littman. 2012. The microbiome in infectious disease and inflammation. *Annu. Rev. Immunol.* 30: 759–795.
32. Alpdogan, O., S. J. Muriglan, J. M. Eng, L. M. Willis, A. S. Greenberg, B. J. Kappel, and M. R. van den Brink. 2003. IL-7 enhances peripheral T cell reconstitution after allogeneic hematopoietic stem cell transplantation. *J. Clin. Invest.* 112: 1095–1107.
33. Alpdogan, S. O., S. X. Lu, N. Patel, S. McGoldrick, D. Suh, T. Budak-Alpdogan, O. M. Smith, J. Grubin, C. King, G. L. Goldberg, et al. 2008. Rapidly proliferating CD44^{hi} peripheral T cells undergo apoptosis and delay posttransplantation T-cell reconstitution after allogeneic bone marrow transplantation. *Blood* 112: 4755–4764.
34. Malmström, V., D. Shipton, B. Singh, A. Al-Shamkhani, M. J. Puklavec, A. N. Barclay, and F. Powrie. 2001. CD134L expression on dendritic cells in the mesenteric lymph nodes drives colitis in T cell-restored SCID mice. *J. Immunol.* 166: 6972–6981.
35. Takeda, I., S. Ine, N. Killeen, L. C. Ndhlovu, K. Murata, S. Satomi, K. Sugamura, and N. Ishii. 2004. Distinct roles for the OX40-OX40 ligand interaction in regulatory and nonregulatory T cells. *J. Immunol.* 172: 3580–3589.
36. Ernst, B., D. S. Lee, J. M. Chang, J. Sprent, and C. D. Surh. 1999. The peptide ligands mediating positive selection in the thymus control T cell survival and homeostatic proliferation in the periphery. *Immunity* 11: 173–181.
37. Goldrath, A. W., and M. J. Bevan. 1999. Low-affinity ligands for the TCR drive proliferation of mature CD8$^+$ T cells in lymphopenic hosts. *Immunity* 11: 183–190.
38. Viret, C., F. S. Wong, and C. A. Janeway, Jr. 1999. Designing and maintaining the mature TCR repertoire: the continuum of self-peptide:self-MHC complex recognition. *Immunity* 10: 559–568.
39. Schluns, K. S., W. C. Kieper, S. C. Jameson, and L. Lefrançois. 2000. Interleukin-7 mediates the homeostasis of naïve and memory CD8 T cells in vivo. *Nat. Immunol.* 1: 426–432.
40. Kieper, W. C., and S. C. Jameson. 1999. Homeostatic expansion and phenotypic conversion of naïve T cells in response to self peptide/MHC ligands. *Proc. Natl. Acad. Sci. USA* 96: 13306–13311.
41. Oehen, S., and K. Brduscha-Riem. 1999. Naive cytotoxic T lymphocytes spontaneously acquire effector function in lymphocytopenic recipients: a pitfall for T cell memory studies? *Eur. J. Immunol.* 29: 608–614.
42. Murali-Krishna, K., and R. Ahmed. 2000. Cutting edge: naive T cells masquerading as memory cells. *J. Immunol.* 165: 1733–1737.
43. Min, B., G. Foucras, M. Meier-Schellersheim, and W. E. Paul. 2004. Spontaneous proliferation, a response of naive CD4 T cells determined by the diversity of the memory cell repertoire. *Proc. Natl. Acad. Sci. USA* 101: 3874–3879.
44. Goldrath, A. W., C. J. Luckey, R. Park, C. Benoist, and D. Mathis. 2004. The molecular program induced in T cells undergoing homeostatic proliferation. *Proc. Natl. Acad. Sci. USA* 101: 16885–16890.
45. Haluszczak, C., A. D. Akue, S. E. Hamilton, L. D. Johnson, L. Pujanauski, L. Teodorovic, S. C. Jameson, and R. M. Kedl. 2009. The antigen-specific CD8$^+$ T cell repertoire in unimmunized mice includes memory phenotype cells bearing markers of homeostatic expansion. *J. Exp. Med.* 206: 435–448.
46. Kieper, W. C., A. Troy, J. T. Burghardt, C. Ramsey, J. Y. Lee, H. Q. Jiang, W. Dummer, H. Shen, J. J. Cebra, and C. D. Surh. 2005. Recent immune status determines the source of antigens that drive homeostatic T cell expansion. *J. Immunol.* 174: 3158–3163.
47. Min, B., H. Yamane, J. Hu-Li, and W. E. Paul. 2005. Spontaneous and homeostatic proliferation of CD4 T cells are regulated by different mechanisms. *J. Immunol.* 174: 6039–6044.
48. Yoshida, H., K. Honda, R. Shinkura, S. Adachi, S. Nishikawa, K. Maki, K. Ikuta, and S. I. Nishikawa. 1999. IL-7 receptor α$^+$CD3$^-$ cells in the embryonic intestine induces the organizing center of Peyer's patches. *Int. Immunol.* 11: 643–655.
49. Worbs, T., U. Bode, S. Yan, M. W. Hoffmann, G. Hintzen, G. Bernhardt, R. Förster, and O. Pabst. 2006. Oral tolerance originates in the intestinal immune system and relies on antigen carriage by dendritic cells. *J. Exp. Med.* 203: 519–527.
50. Murata, K., N. Ishii, H. Takano, S. Miura, L. C. Ndhlovu, M. Nose, T. Noda, and K. Sugamura. 2000. Impairment of antigen-presenting cell function in mice lacking expression of OX40 ligand. *J. Exp. Med.* 191: 365–374.
51. Atarashi, K., T. Tanoue, T. Shima, A. Imaoka, T. Kuwahara, Y. Momose, G. Cheng, S. Yamasaki, T. Saito, Y. Ohba, et al. 2011. Induction of colonic regulatory T cells by indigenous *Clostridium* species. *Science* 331: 337–341.
52. Shinkura, R., K. Kitada, F. Matsuda, K. Tashiro, K. Ikuta, M. Suzuki, K. Kogishi, T. Serikawa, and T. Honjo. 1999. Alymphoplasia is caused by a point mutation in the mouse gene encoding Nf-κb-inducing kinase. *Nat. Genet.* 22: 74–77.

53. Miyawaki, S., Y. Nakamura, H. Suzuka, M. Koba, R. Yasumizu, S. Ikehara, and Y. Shibata. 1994. A new mutation, aly, that induces a generalized lack of lymph nodes accompanied by immunodeficiency in mice. *Eur. J. Immunol.* 24: 429–434.
54. Stenstad, H., A. Ericsson, B. Johansson-Lindbom, M. Svensson, J. Marsal, M. Mack, D. Picarella, D. Soler, G. Marquez, M. Briskin, and W. W. Agace. 2006. Gut-associated lymphoid tissue-primed $CD4^+$ T cells display CCR9-dependent and -independent homing to the small intestine. *Blood* 107: 3447–3454.
55. Matloubian, M., C. G. Lo, G. Cinamon, M. J. Lesneski, Y. Xu, V. Brinkmann, M. L. Allende, R. L. Proia, and J. G. Cyster. 2004. Lymphocyte egress from thymus and peripheral lymphoid organs is dependent on S1P receptor 1. *Nature* 427: 355–360.
56. Chiba, K., Y. Yanagawa, Y. Masubuchi, H. Kataoka, T. Kawaguchi, M. Ohtsuki, and Y. Hoshino. 1998. FTY720, a novel immunosuppressant, induces sequestration of circulating mature lymphocytes by acceleration of lymphocyte homing in rats. I. FTY720 selectively decreases the number of circulating mature lymphocytes by acceleration of lymphocyte homing. *J. Immunol.* 160: 5037–5044.
57. Mandala, S., R. Hajdu, J. Bergstrom, E. Quackenbush, J. Xie, J. Milligan, R. Thornton, G. J. Shei, D. Card, C. Keohane, et al. 2002. Alteration of lymphocyte trafficking by sphingosine-1-phosphate receptor agonists. *Science* 296: 346–349.
58. Sauce, D., M. Larsen, S. Fastenackels, A. Roux, G. Gorochov, C. Katlama, D. Sidi, J. Sibony-Prat, and V. Appay. 2012. Lymphopenia-driven homeostatic regulation of naive T cells in elderly and thymectomized young adults. *J. Immunol.* 189: 5541–5548.
59. Ichii, H., A. Sakamoto, M. Hatano, S. Okada, H. Toyama, S. Taki, M. Arima, Y. Kuroda, and T. Tokuhisa. 2002. Role for Bcl-6 in the generation and maintenance of memory $CD8^+$ T cells. *Nat. Immunol.* 3: 558–563.
60. Min, B., R. McHugh, G. D. Sempowski, C. Mackall, G. Foucras, and W. E. Paul. 2003. Neonates support lymphopenia-induced proliferation. *Immunity* 18: 131–140.
61. Blazar, B. R., A. H. Sharpe, A. I. Chen, A. Panoskaltsis-Mortari, C. Lees, H. Akiba, H. Yagita, N. Killeen, and P. A. Taylor. 2003. Ligation of OX40 (CD134) regulates graft-versus-host disease (GVHD) and graft rejection in allogeneic bone marrow transplant recipients. *Blood* 101: 3741–3748.
62. Sugamura, K., N. Ishii, and A. D. Weinberg. 2004. Therapeutic targeting of the effector T-cell co-stimulatory molecule OX40. *Nat. Rev. Immunol.* 4: 420–431.
63. Croft, M. 2009. The role of TNF superfamily members in T-cell function and diseases. *Nat. Rev. Immunol.* 9: 271–285.
64. Ishii, N., T. Takahashi, P. Soroosh, and K. Sugamura. 2010. OX40-OX40 ligand interaction in T-cell-mediated immunity and immunopathology. *Adv. Immunol.* 105: 63–98.
65. Rose, M. L., D. M. Parrott, and R. G. Bruce. 1976. Migration of lymphoblasts to the small intestine. II. Divergent migration of mesenteric and peripheral immunoblasts to sites of inflammation in the mouse. *Cell. Immunol.* 27: 36–46.
66. Cahill, R. N., D. C. Poskitt, D. C. Frost, and Z. Trnka. 1977. Two distinct pools of recirculating T lymphocytes: migratory characteristics of nodal and intestinal T lymphocytes. *J. Exp. Med.* 145: 420–428.
67. Stagg, A. J., M. A. Kamm, and S. C. Knight. 2002. Intestinal dendritic cells increase T cell expression of $\alpha_4\beta_7$ integrin. *Eur. J. Immunol.* 32: 1445–1454.
68. Iwata, M., A. Hirakiyama, Y. Eshima, H. Kagechika, C. Kato, and S. Y. Song. 2004. Retinoic acid imprints gut-homing specificity on T cells. *Immunity* 21: 527–538.
69. Masopust, D., D. Choo, V. Vezys, E. J. Wherry, J. Duraiswamy, R. Akondy, J. Wang, K. A. Casey, D. L. Barber, K. S. Kawamura, et al. 2010. Dynamic T cell migration program provides resident memory within intestinal epithelium. *J. Exp. Med.* 207: 553–564.
70. Atarashi, K., J. Nishimura, T. Shima, Y. Umesaki, M. Yamamoto, M. Onoue, H. Yagita, N. Ishii, R. Evans, K. Honda, and K. Takeda. 2008. ATP drives lamina propria T(H)17 cell differentiation. *Nature* 455: 808–812.
71. Ivanov, I. I., Rde. L. Frutos, N. Manel, K. Yoshinaga, D. B. Rifkin, R. B. Sartor, B. B. Finlay, and D. R. Littman. 2008. Specific microbiota direct the differentiation of IL-17-producing T-helper cells in the mucosa of the small intestine. *Cell Host Microbe* 4: 337–349.
72. Siddiqui, K. R., S. Laffont, and F. Powrie. 2010. E-cadherin marks a subset of inflammatory dendritic cells that promote T cell-mediated colitis. *Immunity* 32: 557–567.

Y Chromosome–Linked B and NK Cell Deficiency in Mice

Shu-lan Sun,* Satoshi Horino,* Ari Itoh-Nakadai,† Takeshi Kawabe,* Atsuko Asao,* Takeshi Takahashi,‡ Takanori So,* Ryo Funayama,§ Motonari Kondo,¶ Hirotomo Saitsu,‖ Naomichi Matsumoto,‖ Keiko Nakayama,§ and Naoto Ishii*

There are no primary immunodeficiency diseases linked to the Y chromosome, because the Y chromosome does not contain any vital genes. We have established a novel mouse strain in which all males lack B and NK cells and have Peyer's patch defects. By 10 wk of age, 100% of the males had evident immunodeficiencies. Mating these immunodeficient males with wild-type females on two different genetic backgrounds for several generations demonstrated that the immunodeficiency is linked to the Y chromosome and is inherited in a Mendelian fashion. Although multicolor fluorescence in situ hybridization analysis showed that the Y chromosome in the mutant male mice was one third shorter than that in wild-type males, exome sequencing did not identify any significant gene mutations. The precise molecular mechanisms are still unknown. Bone marrow chimeric analyses demonstrated that an intrinsic abnormality in bone marrow hematopoietic cells causes the B and NK cell defects. Interestingly, fetal liver cells transplanted from the mutant male mice reconstituted B and NK cells in lymphocyte-deficient *Il2rg*$^{-/-}$ recipient mice, whereas adult bone marrow transplants did not. Transducing the EBF gene, a master transcription factor for B cell development, into mutant hematopoietic progenitor cells rescued B cell but not NK cell development both in vitro and in vivo. These Y chromosome–linked immunodeficient mice, which have preferential B and NK cell defects, may be a useful model of lymphocyte development.
***The Journal of Immunology*, 2013, 190: 6209–6220.**

Most primary immunodeficiencies are inherited disorders. For example, mutations of the common cytokine receptor γ-chain (*Il2rg*) gene, which is located on the X chromosome, cause X-linked SCID, which is characterized by T and NK cell deficiencies and functionally impaired mature B cells. Mutations of the recombinase-activating genes *Rag1* and *Rag2* induce T and B cell deficiencies while retaining functional NK cells. These immunodeficiencies are caused by gene mutations on an autosome or an X chromosome (1, 2). No hereditary Y chromosome–linked immunodeficiencies have been reported in humans.

The Y chromosome is one of two chromosomes that pair with the X chromosome and determine sex in most mammals. The mouse Y chromosome is 16-Mb long and contains 54 genes; the human Y chromosome is 58-Mb long and encodes 86 genes. It is apparent that Y chromosomes do not contain genes essential for life, because females do not have the Y chromosome. Only two studies showed the male mice–specific disorder that is Y chromosome linked. One is Yaa (Y-linked autoimmune accelerator). Yaa mice develop a disease similar to systemic lupus erythematosus, and the incidence and onset are much higher in males than in their female littermates in certain mouse strains, including BXSB and MLR (3). Recent studies have shown that in Yaa mice, the part of the X chromosome pseudoautosomal region containing the *TLR7* gene is translocated onto the Y chromosome. Therefore, the duplication of TLR7, which may render B cells hypersensitive to self-Ags containing RNA, contributes to the BXSB strain's Y-linked autoimmune-prone phenotype. However, the *Yaa* mutation alone is not sufficient to induce autoimmune disease in C56BL/6 male mice; additional genetic mutations are required. In this context, the autoimmune disease associated with the *Yaa* mutation is not a Y-chromosomal Mendelian disease. Another study showed a mouse strain in which Vα14i NKT cell is absent in the male mice (4). However, they did not analyze the Y chromosome, so the mechanism of Y chromosome–linked NKT deficiency is still unknown.

B cells are lymphocytes that play a large role in humoral immune responses. Murine B cell development is initiated in the fetal liver cells and relocates to the bone marrow after birth. B cell development requires the coordinated efforts of transcription factors and cytokines, particularly IL-7 (5). IL-7 regulates early B cell transcription factor (EBF) expression in the adult bone marrow (6). EBF is a B cell–specific transcription factor that regulates crucial genes affecting B cell development, such as *λ5*, *Vpre B*, and *mb-1* (7, 8). EBF cooperates with E2A to positively regulate Pax5 expression. These transcription factors, along with PU.1, are indispensable for B cell development (9–11).

NK cells are a distinct lymphocyte subset with a central role in innate immunity (12). Early studies suggested that NK cells, like B cells and myeloid-lineage cells, develop primarily in the bone marrow. NK precursor (NKP) cells derived from hematopoietic stem cells (HSCs) give rise to immature NK (iNK) and then

*Department of Microbiology and Immunology, Tohoku University Graduate School of Medicine, Sendai 980-8575, Japan; †Department of Biochemistry, Tohoku University Graduate School of Medicine, Sendai 980-8575, Japan; ‡Central Institute for Experimental Animals, Kawasaki 210-0821, Japan; §Department of Cell Proliferation, Tohoku University Graduate School of Medicine, Sendai 980-8575, Japan; ¶Department of Immunology, Toho University School of Medicine, Tokyo 143-8540, Japan; and ‖Department of Human Genetics, Yokohama City University Graduate School of Medicine, Yokohama 236-0004, Japan

Received for publication January 31, 2013. Accepted for publication April 19, 2013.

This work was supported in part by a grant-in-aid for scientific research on priority areas from the Ministry of Education, Science, Sports and Culture of Japan, a grant-in-aid for scientific research on priority areas from the Japan Society for the Promotion of Science, and grants from the Japan Science and Technology Agency, the Sumitomo Foundation, the Uehara Memorial Foundation, the Novartis Foundation for the Promotion of Science, and the Yakult Bio-Science Foundation.

Address correspondence and reprint requests to Prof. Naoto Ishii, Department of Microbiology and Immunology, Tohoku University Graduate School of Medicine, 2-1 Seiryo-machi, Aoba-ku, Sendai 980-8575, Japan. E-mail address: ishiin@med.tohoku.ac.jp

Abbreviations used in this article: E, embryonic day; EBF, early B cell transcription factor; FISH, fluorescence in situ hybridization; HPC, hematopoietic progenitor cell; iNK, immature NK; NKP, NK precursor; PP, Peyer's patch; SCF, stem cell factor.

www.jimmunol.org/cgi/doi/10.4049/jimmunol.1300303

mature NK cells. Several transcription factors, such as Ets-1, Id2, PU.1, Ikaros, T-bet, E4BP4, and Irf-2 are required for NK cell maturation (12–14). Among these, PU.1, Ikaros, and Ets-1 are critical for generating NKPs, and the other factors become involved after cells are committed to the NK cell lineage. For example, *Id2*$^{-/-}$ mice have normal numbers of NKP and iNK cells but significantly fewer mature NK cells (15). However, these factors are not necessarily specific to the NK lineage, because their individual deletions sometimes cause defects in other hematopoietic cell lineages.

In this study, we established a novel immunodeficient mouse strain characterized by Y chromosome–linked hereditary B and NK cell deficiencies. B and NK cells gradually diminished after 3 wk of age and disappeared by 10 wk of age in 100% of the males of this strain. B cell development was arrested at the prepro-B cell stage, and NKP cells were almost undetectable in these mutant mice. Although intensive genomic analyses failed to reveal the precise molecular mechanisms of this Y-linked lymphocyte deficiency, the mouse phenotype suggests that a mutation of one gene may cause B and NK cell deficiency without affecting T cell development. Therefore, this novel mouse strain may be a useful model for distinguishing the developmental processes of B, T, and NK cells, which are thought to derive from common lymphoid progenitor cells.

Materials and Methods

Mice

B cell–deficient mice on a C57BL/6N background were bred and maintained under specific pathogen-free conditions. Unless otherwise indicated, age-matched (3–20 wk old) and female littermates were used as controls. All procedures were performed according to protocols approved by Tohoku University's Institutional Committee for the Use and Care of Laboratory Animals.

Flow cytometry

Single-cell suspensions were prepared and cells immunostained as previously described (16). Dead cells were positively stained by propidium iodide and excluded from analysis. Lymphocyte suspensions from the spleen, bone marrow, peripheral blood, and fetal liver were incubated with a CD16/32 mAb (2.4G2) and stained for 30 min on ice with a combination of the following mouse-specific Abs: FITC-CD19 (6D5; BioLegend, San Diego, CA), PE–anti-IgM (eB121-15F9; eBioscience, San Diego, CA), PE-CD3 (eBio500A2; eBioscience), Pacific Blue-CD4 (RM4-5; BD Pharmingen, San Diego, CA), allophycocyanin-CD8 (53-6.7; BioLegend), FITC-CD11b (M1/70; BD Pharmingen), PE–anti-NK1.1 (PK136; BD Pharmingen), allophycocyanin–anti-B220 (RA3-6B2; BioLegend), FITC-CD90.2 (53-2.1; BD Pharmingen), FITC-CD43 (S7; BD Pharmingen), PE–anti-Ly5.1 (6c3; BioLegend), Pacific Blue-CD24 (M1/69; BioLegend), FITC-CD34 (RAM34; BD Pharmingen), allophycocyanin-CD117 (2B8; BioLegend), PE/Cy7–anti-Sca-1 (D7; BioLegend), Biotin-CD127 (A7R34; BioLegend), Biotin-CD122 (TM-β1; BioLegend), PE-CD5 (53-7.3; BD Pharmingen), FITC–Gr-1 (RB6-8C5; BD Pharmingen), PE-Ter119 (TER119; BioLegend), FITC-CD71 (RI7217; BioLegend), allophycocyanin-CD3 (145-2c11; BioLegend), and PE–anti-IgM (eB121-15F9; eBioscience). Biotinylated Abs were visualized by BD Horizon V450 streptavidin (BD Pharmingen). Samples were analyzed with an FACSCanto II or LSRFortessa system (BD Biosciences); data were analyzed with FlowJo flow cytometry analysis software (Tree Star).

Radioactive proliferation assay

Splenic T cells were first separated by CD90.2 Microbeads (Miltenyi Biotec, Bergisch Gladbach, Germany). A total of 1×10^5 cells was then seeded in the wells of a 96-well plate precoated with 10 μg/ml anti-mouse CD3e mAb (145-2C11) in a RPMI 1640 containing 10% FCS, 200 U/ml streptomycin, 200 U/ml penicillin, 50 μM 2-ME, and 1 μg/ml anti-mouse CD28 mAb. After 48 h stimulation, 1 μCi/well [^{3}H]thymidine was added, and the incorporation of [^{3}H]thymidine was measured by a γ-scintillation counter.

Real-time PCR

Prepro-B ($B220^+CD43^-CD24^-Ly51^-$) cells were purified from bone marrow cells using an FACSAria II cell sorter (BD Biosciences) and lysed with 1 ml TRIzol reagent (Invitrogen, Carlsbad, CA). Total RNA was purified from the cells. The cDNA was then synthesized with SuperScript Reverse Transcriptase and Random Primers (Invitrogen). The cDNA was then amplified over 40 cycles on a 7500 Real-time PCR system using SYBR Premix EXtaq (TaKaRa Bio, Shiga, Japan), ROX Reference DyeII (TaKaRa Bio), and primer sets. All samples were normalized to GAPDH. The PCR primers for E12, E47, EBF, PU.1, Id2, Ikaros, and GAPDH were as follows: E12 forward, 5′-GGGAGGAGAAAGAGGATGA-3′ and reverse, 5′-GCTCCGCCTTCTGCTCTG-3′; E47 forward, 5′-GGGAGGAGAAAGAGGATGA-3′ and reverse, 5′-CCGGTCCCTCAGGTCCTTC-3′; PU.1 forward, 5′-GAACAGATGCACGTCCTCGAT-3′ and reverse, 5′-GGGGACAAGGTTTGATAAGGGAA-3′; EBF forward, 5′-CTACAGCAATGGGATACGGAC-3′; reverse, 5′-TTTCAGGGTTCTTGTCTTGGC-3′; Id2 forward, 5′-CTCCAAGCTCAAGGAACTGG-3′ and reverse, 5′-ATTCAGATGCCTGCAAGGAC-3′; Ikaros forward, 5′-TGTGTCATCGGAGCGAGAG-3′ and reverse, 5′-GGAAGGCATCCTGCGAGTT-3′; and GAPDH forward, 5′-CCAGGTTGTCTCCTGCGACTT-3′ and reverse, 5′-CCTGTTGCTGTAGCCGTATTCA-3′.

Adoptive cell transfer

Bone marrow cells were extracted by a pressurized flow of sterile tissue-culture medium through femurs and tibias dissected from donor mice. Fetal liver cells were taken from female or male mice at embryonic day (E) 17.5. Recipient *Il2rg*$^{-/-}$ mice were irradiated with 5 Gy, and on the following day, 4×10^6 adult bone marrow cells or fetal liver cells were transplanted into recipients via the tail vein.

Purification of hematopoietic progenitor cells from bone marrow and fetal liver

Hematopoietic progenitor cells (HPCs) were purified from adult bone marrow or E17.5 fetal liver cells by staining with the following mouse-specific, biotinylated lineage markers: CD3, B220, TER119, Gr1, DX5, and CD11b. HPCs were negatively separated by anti-Biotin MicroBeads with auto MACS Columns (Miltenyi Biotec).

In vitro lymphopoiesis

HPCs collected from adult bone marrow or E17.5 fetal liver cells were cultured on OP9 stromal cells in α-MEM medium containing 20% FCS, 200 U/ml streptomycin, 200 U/ml penicillin, and 50 μM 2-ME or 7 d. For B cell development, the medium was supplemented with 5 ng/ml stem cell factor (SCF), 5 ng/ml Flt3 ligand, and 10 ng/ml IL-7; for NK cells, the medium was supplemented with 5 ng/ml SCF, 5 ng/ml Flt3 ligand, and 30 ng/ml IL-15.

Retroviral transduction

We produced a virus from a packaging cell line, PLAT-E, by transiently transfecting the MSCV-EBF-IRES-GFP plasmid (6) and MSCV-IRES-GFP as control using FuGENE transfection reagent (Roche, Madison, WI). HPCs from males (Ly5.2) or female littermates (Ly5.2) were cultured in RPMI 1640 containing 10% FCS, 200 U/ml streptomycin, 200 U/ml penicillin, and 50 μM 2-ME supplemented with mouse recombinant SCF (50 ng/ml), IL-6 (10 ng/ml), IL-3 (5ng/ml), FLT-3 ligand (5 ng/ml), and IL-7 (5 ng/ml). On the following day, the cells were transferred onto a RetroNectin-coated (TaKaRa Bio) plate in the presence of retroviral supernatant. For spin infection, the plate was centrifuged at $2000 \times g$ at 32°C for 2 h once daily on days 1 and 2. Two days postinfection, the cells were washed and then transferred into irradiated Ly5.1 wild-type mice or cocultured on OP9 cells under B or NK cell differentiation conditions.

Statistical analysis

Statistical analysis was performed by Student *t* test. The *p* values < 0.05 were considered significant.

Results

Mutant male mice lack NK and B cells and Peyer's patches

In our mouse population, a novel mutant strain emerged spontaneously, in which all males lacked Peyer's patches (PP) and mated these males with wild-type female mice, we observed their offspring for the presence or absence of PPs. Although PPs in both the male and female offspring were visible from 4 to 6 wk after birth, PPs were completely lacking in the male offspring as they grew up to 10 wk old (Fig. 1A and data not shown). This indicated

that the early PP compartmentalization process was normal in the male mice. Moreover, each male mouse had a normal number of lymph nodes, although the lymph nodes were abnormally small, and was outwardly normal in behavior, fertility, and appearance. To understand the characteristic of these mutant male mice, we analyzed hematopoietic cells in the spleen, peritoneal cavity, thymus, bone marrow, and peripheral blood. Interestingly, the males had virtually no B (B1 and B2) cells and also had significantly fewer NK cells ($NK1.1^+CD3^-$) than their female littermates (Fig. 1B, 1C). NK deficiency was also confirmed with a different NK cell marker ($CD3^-DX5^+FcR\varepsilon I^-$) (data not shown). However, there were no differences in the absolute cell number of myeloid and erythroid populations in the bone marrow or of RBCs in the periphery (Fig. 1B, 1F, 1G). In addition, the absolute

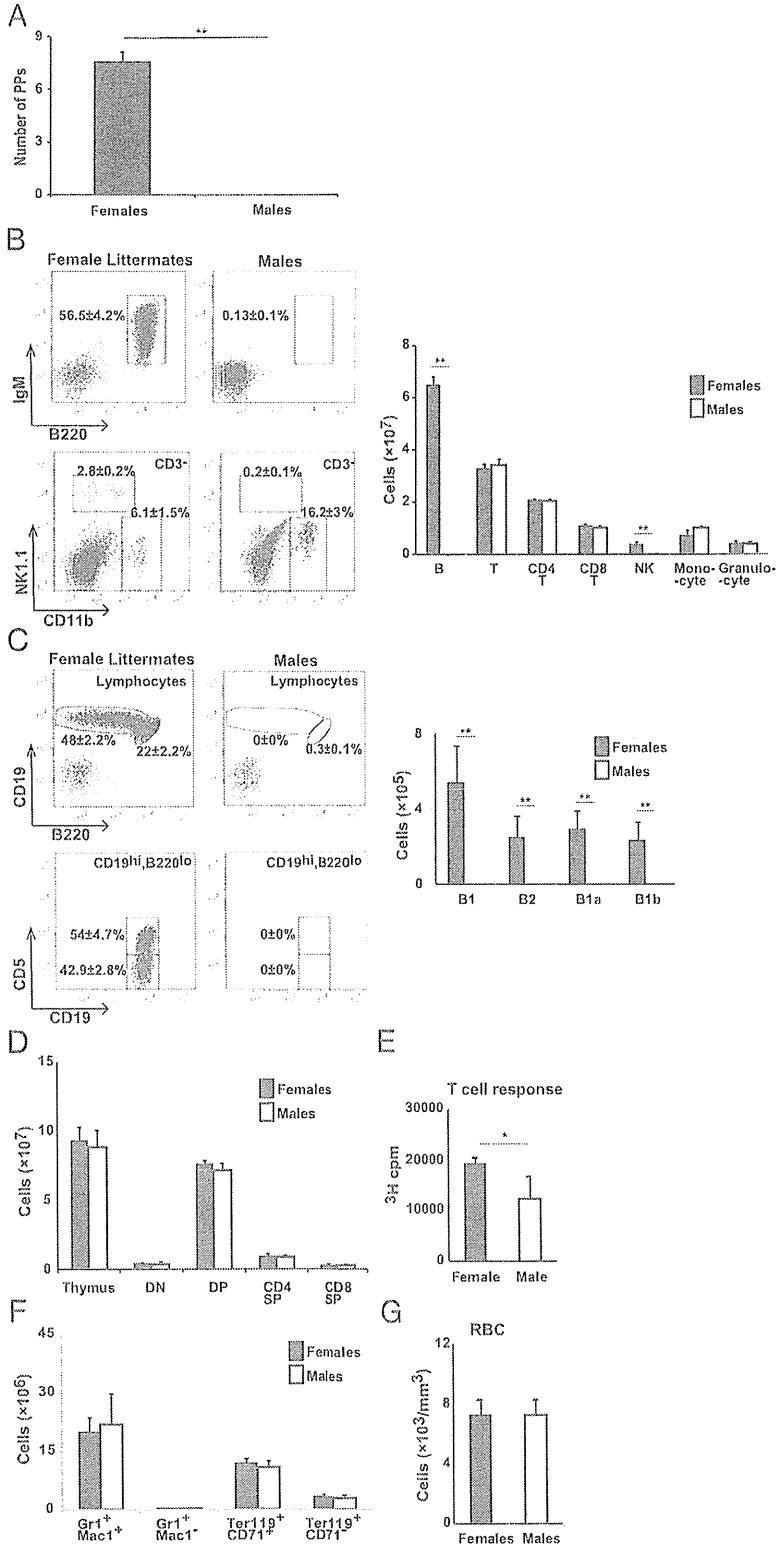

FIGURE 1. Mutant male mice specifically lack PPs. (**A**) Number of PPs on small intestines of 12-wk-old males or their female littermates. Frequency and the absolute number of hematopoietic lineages in the spleen (**B**), peritoneal cavity (**C**), thymus (**D**), and bone marrow (**F**) were analyzed by flow cytometry. $B220^+IgM^+$ B cell, $CD3^+$ T cell, $CD3^+CD4^+$ T cell, $CD3^+CD8^+$ T cell, $NK1.1^+CD3^-$ NK cell, $CD11b^+$ monocyte, and $Gr\text{-}1^+$ granulocyte populations are shown. (C) Peritoneal lymphocytes were separated into the following subsets: total B1, $CD19^+B220^{lo\text{-}int}$; B1a, $CD19^+B220^{lo\text{-}int}$ $D5^+$; and B1b, $CD19^+B220^{lo\text{-}int}$ $CD5^{lo/-}$. (D) Thymic cells were stained with CD4 and CD8 and separated into the following subsets: double-negative (DN), $CD4^-CD8^-$; double-positive (DP), $CD4^+CD8^+$; CD4 single-positive (SP), $CD4^+CD8^-$; and CD8 SP, $CD4^-CD8^+$. (**E**) Splenic T cells were stimulated with anti-CD3 and anti-CD28 mAbs for 4–8 h and then pulsed with [^{3}H]thymidine. The incorporation of [^{3}H]thymidine was measured. (F) Myeloid cells ($Gr1^+Mac1^+$ and $Gr1^+Mac1^-$), $Ter119^+CD71^+$ nucleated erythroid progenitors, and $Ter119^+$ $D71^-$ nonnucleated erythroid cells in the bone marrow were counted. (**G**) RBCs in the peripheral blood were counted. Numbers in FACS plots indicate the percentages relative to the gated cells. Data are from more than five experiments (A–D) or one experiment (E–G) with at least four mice per genotype. Error bars indicate SD (± SD). $*p < 0.05$, $**p < 0.01$.

number of T cell subsets in the thymus and spleen was comparable between the mutant males and the female littermate controls (Fig. 1B, 1D), suggesting normal T cell development in the mutant male mice. When splenic T cells were stimulated with anti-CD3ε mAb, the proliferative responses of T cells in the mutant male mice were clearly observed but significantly lower than female controls' (Fig. 1E).

B and NK cell deficiency is inherited in a Mendelian, Y chromosome–linked fashion

Because all male pups in this strain were B and NK cell deficient, we hypothesized that the phenotype might be inherited as a dominant trait linked to the Y chromosome. To confirm this, we mated PP (B and NK cell)–deficient male mice with wild-type female mice on a C57BL/6 (Fig. 2A, *left panel*) or BALB/c (Fig. 2A, *right panel*) background, and looked for PPs (B and NK cell) in their 10-wk-old offspring. All male offspring of a mutant male parent also lacked PPs (B and NK cells). In contrast, there was no abnormality in PPs or B cells in the female offspring or in males that inherited their Y chromosome from a wild-type male. The family tree indicated that the B and NK cell deficiency was inherited in a Mendelian fashion linked to the Y chromosome.

To determine the Y chromosome's genetic abnormality, we examined it by fluorescence in situ hybridization (FISH) analysis. The Y chromosome in the mutant males (n = 10) was one third shorter than that in wild-type male mice, suggesting a structural abnormality (Fig. 2B).

The Yaa mutation, which contributes to a higher incidence of autoimmune disease in male than in female BXSB mice, is caused by the novel translocation of a gene locus from the X chromosome onto the Y chromosome, resulting in the duplication of several genes. To look for duplication or copy-number abnormalities of certain genes in our B and NK cell–deficient male mice, we performed array-based comparative genomic hybridization with spleen cells and hepatic cells from mutant male and wild-type male mice on the same genetic background. We found gene-copy abnormalities of three autosomal gene loci (data not shown). However, FISH analysis with bacterial artificial chromosome clone probes derived from these three autosomal gene loci failed to find any evidence of an insertion or translocation of the loci into the Y chromosome (data not shown).

We also sequenced Y chromosome exomes from B and NK cell–deficient and wild-type male mice (n = 3 each) from the same B6 strain. However, we could not find any significant nucleotide differences, including single nucleotide polymorphisms, between the Y chromosome exons in mutant and wild-type mice (data not shown). Thus, the genetic Y chromosome abnormality responsible for the Y chromosome–linked immunodeficiency remains unclear.

B and NK cell populations in the mutant male mice decrease with age

B and NK cells were absent in the adult male mice of this strain. To examine whether B or NK cell lymphopenia occurs at birth, we measured the numbers of B and NK cells in the bone marrow, spleen, lymph nodes, and peripheral blood at 3, 6, 8, and 12 wk of age. The B and NK cell populations in males at 3 wk of age were comparable with those in females, but had decreased to a markedly lower level at 6 wk of age (Fig. 3A). Interestingly, B1 cells in the males were markedly reduced compared with those in the female littermates even at 3 wk after birth and completely disappeared by 12 wk of age (Fig. 3B). Consistent with B cell decline, serum IgG and IgM dramatically decreased at 6 wk of age (Fig. 3D). In contrast, T cells increased with age in both males and females and

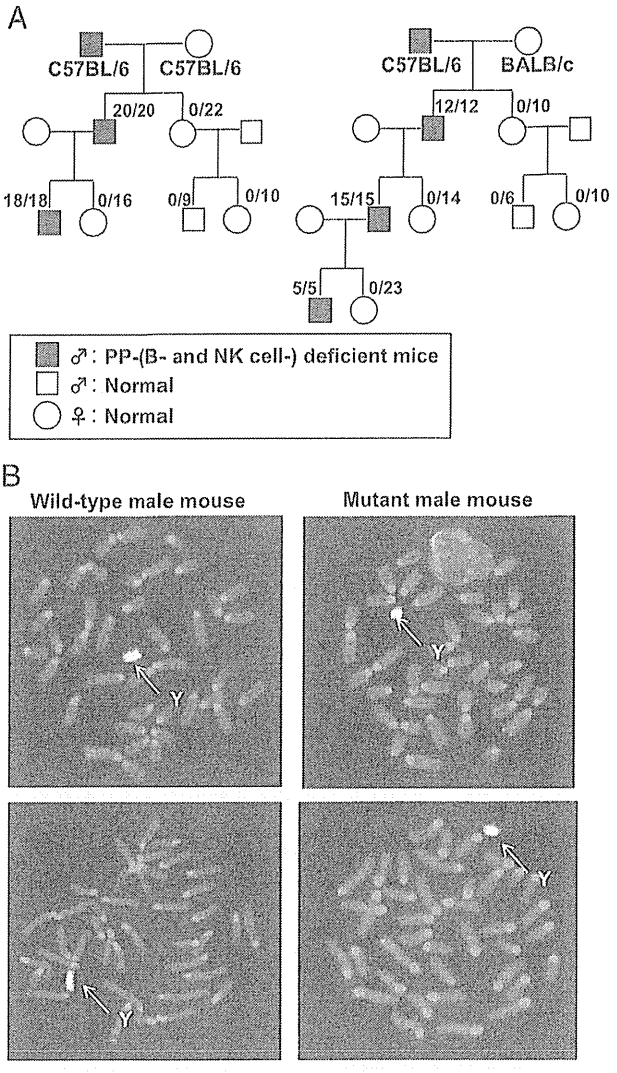

FIGURE 2. B and NK cell deficiency is inherited in a Mendelian fashion linked to the Y chromosome. (**A**) B cell–deficient male mice were mated with C57BL/6 (*left panel*) or BABL/c (*right panel*) wild-type female mice for several generations. The 10-wk-old offspring were then examined for B and NK cells in the peripheral blood and for PPs. Mice deficient in PPs (B and NK cells) are represented by filled symbols and unaffected individuals by open symbols (squares, males; circles, females). The numbers of immunodeficient mice/number of offspring are shown. (**B**) Y chromosomes from wild-type and B and NK cell–deficient males were analyzed by FISH. The Y chromosome is presented in yellow; pictures show Y chromosomes from different cells. Representative results are shown (n = 20 cells each).

the thymic development of T cells in the males was normal (Fig. 3A, 3C).

To rule out the possibility that androgenic hormones were associated with this phenotype, we compared splenic B and T cells in 10-wk-old B cell–deficient males that had been either castrated or subjected to a sham operation at 2 wk of age (Fig. 3D). The castrated male mice lacked B cells but had normal T cells, indicating that the male-specific B cell defect was independent of androgen.

Bone marrow lymphopoiesis in the mutant male mice is arrested at the prepro-B to pro-B cell transition

Because B cells were depleted in the adult male mutant mice, we looked at various stages of B cell differentiation to determine which stage was arrested. The B cell development from HSCs is sub-

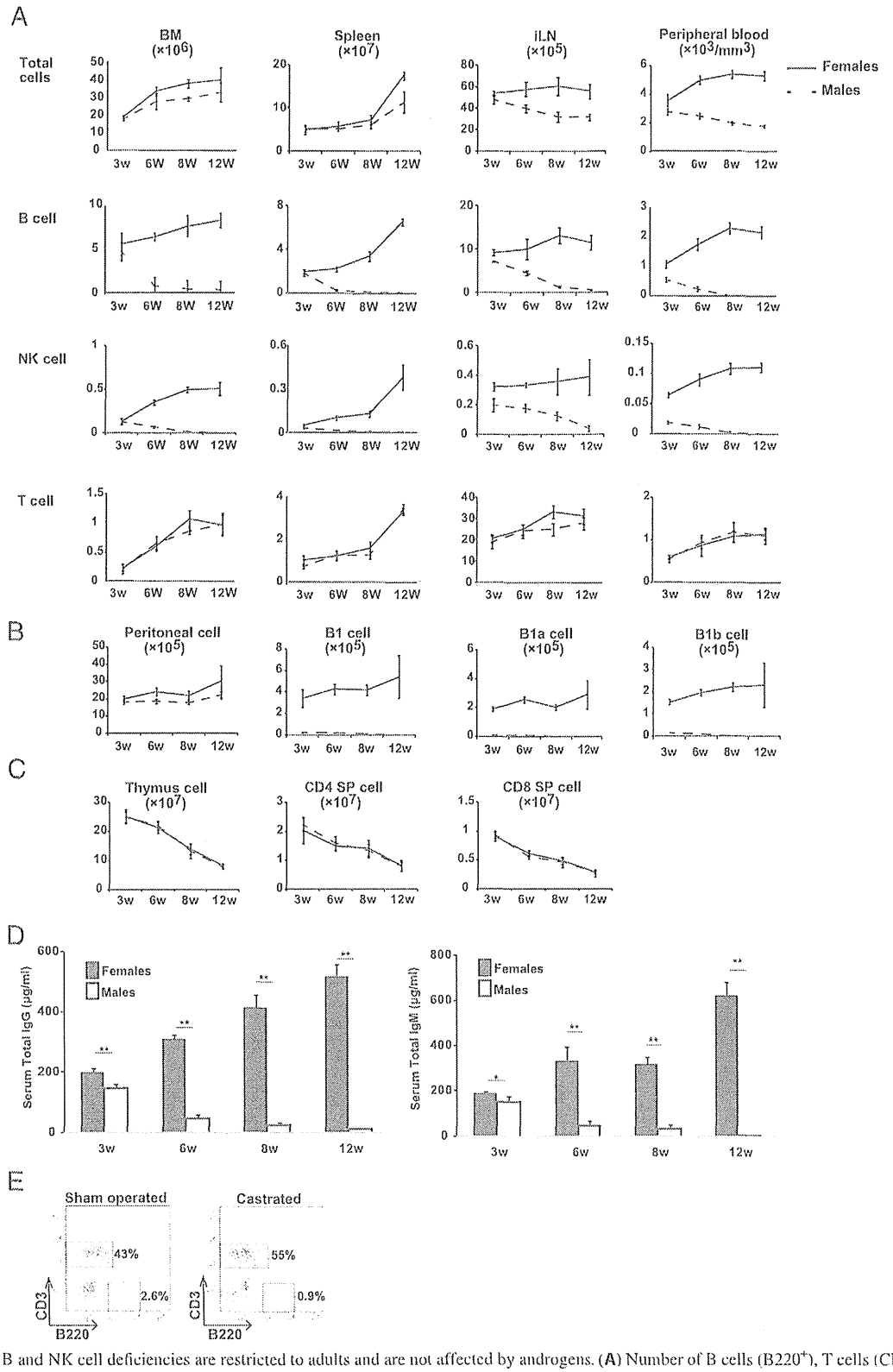

FIGURE 3. B and NK cell deficiencies are restricted to adults and are not affected by androgens. (**A**) Number of B cells ($B220^+$), T cells ($CD3^+$), and NK cells ($NK1.1^+$ $CD3^-$) from the bone marrow, spleen, inguinal lymph nodes (iLN), and blood. Numbers of B cell subsets in the peritoneal cavity (**B**) and number of T cell subset in the thymus (**C**) of male and female littermates at 3, 6, 8, and 12 wk of age. (**D**) Serum levels of IgG and IgM in 3-, 6-, 8-, and 12-wk-old mice were calculated from absorbance at 450 nm (A_{450}). Data are from one experiment ($n = 4$ mice/genotype). Error bars indicate SD (± SD). (**E**) The 2-wk-old male offspring of B cell–deficient male mice were castrated or subjected to a sham operation, and then the percentages of B and T cells in the spleen were compared at 10 wk of age. Data are from one experiment ($n = 2$ mice/group). $^*p < 0.05$, $^{**}p < 0.01$.

divided into Hardy fractions A–F (17). We found decreased numbers of B cell progenitors in the bone marrow that had undergone the transition from prepro-B to pro-B cells, corresponding to the Hardy fractions A ($B220^+CD43^+BP\text{-}1^-CD24^-$) and B ($B220^+CD43^+BP\text{-}1^-CD24^+$). Immature B cells, corresponding to Hardy fraction E ($B220^+CD43^-IgM^-IgD^+$), were severely deficient (Fig. 4A, 4B).

NK cells are lost in the mutant male mice

NK cells, which develop primarily in the bone marrow, are derived from HSCs via NKP and iNK cells. Because the very low number of splenic NKs in the mutant males suggested defective NK development, we compared the number of NKP and iNK cells in the bone marrow of males and their female littermates. The numbers of both NKP ($CD11b^-CD3^-NK1.1^-CD122^+$) and iNK ($CD11b^-CD3^-NK1.1^+CD122^+$) cells were substantially reduced in the male mice (Fig. 4C, 4D), suggesting that NK cell development was impaired in the males.

Abnormal expression of Sca-1 on hematopoietic cells in the bone marrow

We further examined the lymphoid, myeloid, and erythroid progenitor populations in the bone marrow of the mutant male mice. As shown in Fig. 5, it appeared that progenitor cells (defined as $lineage^-c\text{-}Kit^{hi}$ and $Sca\text{-}1^-$) of all of the indicated lineages in the mutant males were markedly reduced. However, Fig. 1B and 1F showed normal number of mature myeloid and erythroid cells in the mutant male mice. Interestingly, most $lineage^-$ cells in the mutant males strongly expressed the Sca-1 marker (*top panels* of Fig. 5A), which is commonly used to define the hematopoietic

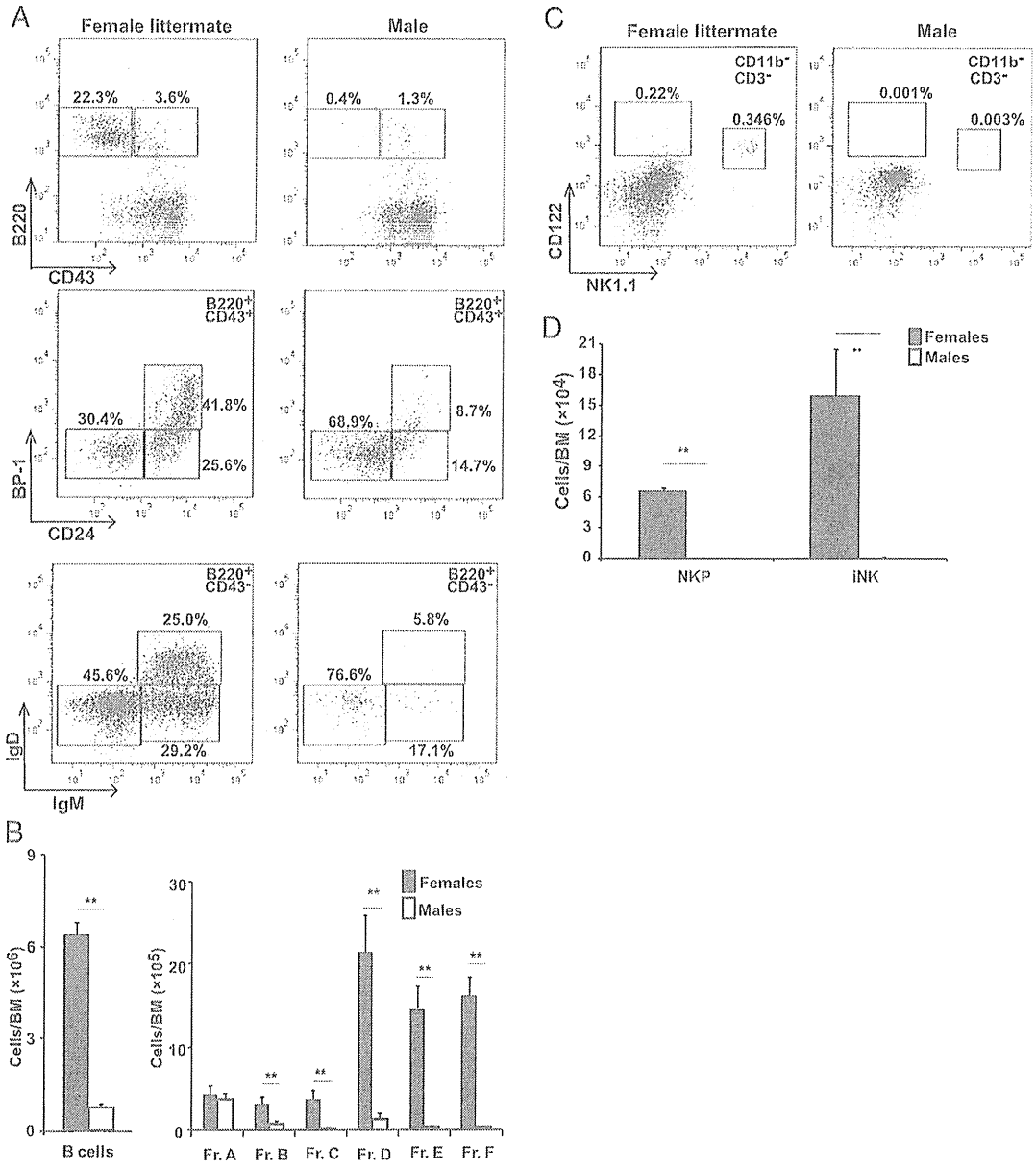

FIGURE 4. B and NK cell developments are arrested. Frequency (**A**) and number (**B**) of B cell subsets in the bone marrow at 6 wk of age. Hardy fractions in the bone marrow were gated as follows: $B220^+CD43^+BP\text{-}1^-CD24^-$ (A); $B220^+CD43^+BP\text{-}1^-CD24^+$ (A); $B220^+CD43^+BP\text{-}1^+CD24^+$ (A); $B220^+CD43^-IgM^-IgD^-$ (A); $B220^+CD43^-IgM^+IgD^-$ (A; and $B220^+CD43^-IgM^+IgD^+$ (B); the C' fraction ($B220^+CD43^+BP\text{-}1^+CD24^{hi}$) was not resolved. Data are representative from three independent experiments of five mice per genotype. Frequency (**C**) and number (**D**) of NKp ($CD122^+CD3^-CD11b^-NK1.1^-$) and iNK cells ($CD122^+NK1.1^+CD3^-CD11b^-$) are shown. Data are representative of four or five mice per genotype. $^{**}p < 0.01$.

progenitor or stem cells. Therefore, due to abnormally high expression of Sca-1, we may have been unable to exactly evaluate the hematopoietic progenitor cells in the mutant male mice.

The failure of adult B and NK lymphopoiesis is cell intrinsic

B cells and NK cells can be produced from bone marrow cells cultured in vitro on stromal cells, such as OP9 cells, in the presence of IL-7 or IL-15 (18, 19). To determine the cellular origin of the phenotype of the male mutant mice, we isolated HPCs, identified as Lin$^-$ (B220$^-$, Thy1$^-$, DX5$^-$, Ter119$^-$, Gr-1$^-$, CD11b$^-$) bone marrow cells, from the male mice and their female littermates. The HPCs were cultured on OP9 cells, with subsequently added cytokines. HPCs derived from the bone marrow of males did not produce NK (NK1.1$^+$) cells or B (CD19$^+$) cells, whereas significant NK and B cell populations were generated from the HPCs from female littermates (Fig. 6A).

To confirm this cell-intrinsic abnormality in vivo, we conducted bone marrow chimera experiments by transfusing a mixture of equal parts of wild-type (Ly5.1$^+$) and mutant (Ly5.2$^+$) bone marrow cells into lymphocyte-deficient *Il2rg*$^{-/-}$ mice. Consistent with the in vitro results, Ly5.2$^+$ bone marrow cells of mutant males failed to produce B or NK cells, whereas Ly5.1$^+$ wild-type HPCs fully reconstituted both B and NK cells in the same recipient mice (Fig. 6B). Transplanting wild-type bone marrow cells into irradiated mutant male mice rescued the B and NK cell deficiency (Fig. 6C), and PPs were also recovered 10 wk after the transplant (data not shown). This suggests that the PP deficiency is a result of the B cell deficiency and not an anlage defect. These results clearly indicate that the defect of B and NK cells in the mutant mice was intrinsic to hematopoietic cells.

Interestingly, the in vitro lymphopoiesis of B and NK cells from fetal liver HPCs was the same whether the HPCs were from the mutant males or their female littermates (Fig. 7A). Furthermore, the male fetal liver cells reconstituted B and NK cells in vivo, although at a lower level than cells from female littermates (Fig. 7B). Because fetal liver progenitors from the mutant males could produce B and NK cells, we compared the fetal B cell subsets and NK lymphopoiesis in male and female littermates at E17.5, when IgM$^+$ B cells and iNK are already present in wild-type mice (20, 21). As expected, we did not find a significant difference in the frequency of B or NK cells in the fetal liver of male and female littermate embryos (Fig. 7C). However, both B and NK cells derived from the male fetal liver disappeared by 10 wk after transplantation (data not shown). Nevertheless, the above results provide further evidence that the fetal B and NK cell development in the males was intact and that the NK and B cells detected in 3-wk-old males were generated from fetal liver progenitors.

In addition, male fetal liver cells could produce these lymphocytes even in male recipients (data not shown), supporting the conclusion that androgen does not contribute to the defect of B and NK cells in these mutant male mice.

EBF restores the precursor cells' ability to generate B220$^+$ B cells in mutant males

To address the molecular mechanisms for arresting the B cell development, we isolated prepro-B cells (Hardy fraction A) from the

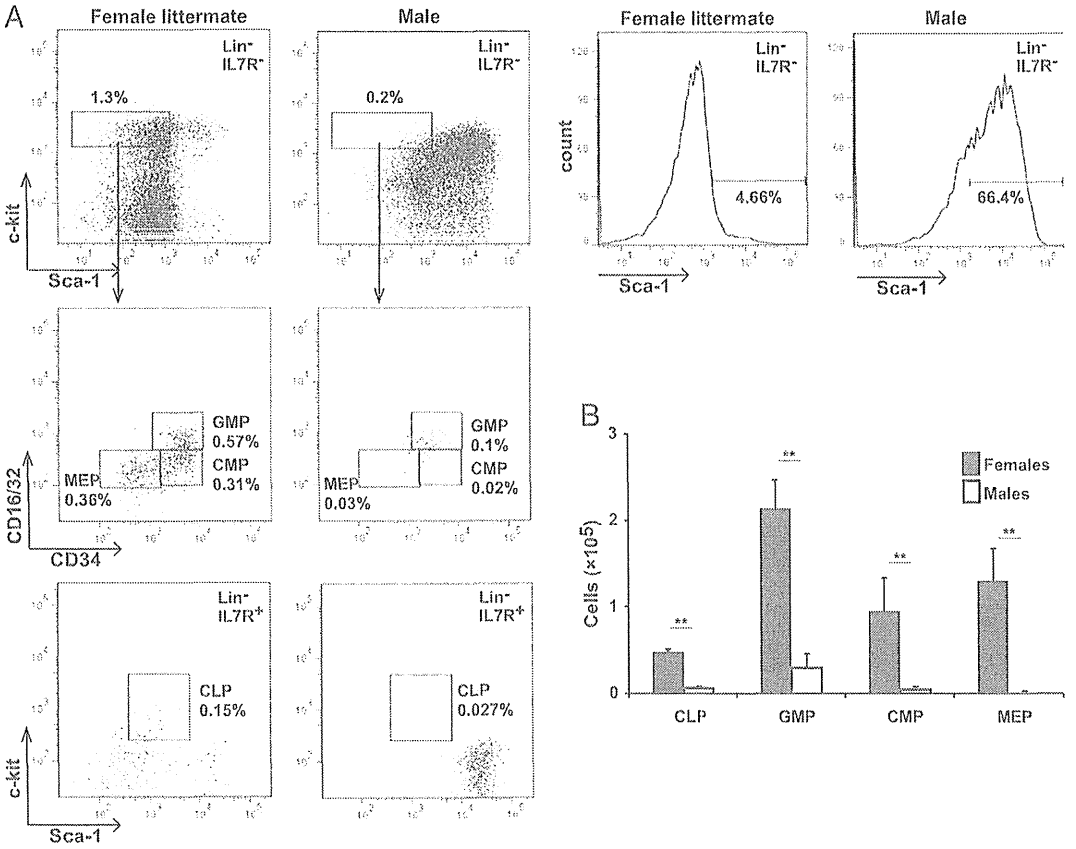

FIGURE 5. Abnormally high expression of Sca-1 on hematopoietic cells in the bone marrow. (**A**) Representative FACS analysis with the bone marrow cells from 12-wk-old mice are shown. Numbers in the FACS plots indicate the percentages of the indicated populations among total bone marrow cells. Each progenitor population was defined as bellow. The histogram shows expression of Sca-1 related to Lin$^-$CD127$^-$ gated cells. (**B**) The average absolute numbers of the indicated populations in the bone marrow are shown ($n = 3$ each). CLP: Lin$^-$CD127$^+$Sca1^{lo}c-Kit^{lo}; CMP: Lin$^-$CD127$^-$c-Kit^{hi}Sca1$^-$CD34$^{+/lo}$CD16/32^{int}; GMP: Lin$^-$CD127$^-$c-Kit^{hi}Sca1$^-$CD34$^+$CD16/32$^+$; and MEP: Lin$^-$CD127$^-$c-Kit^{hi}Sca1$^-$CD34$^-$CD16/32$^-$. $^{**}p < 0.01$.

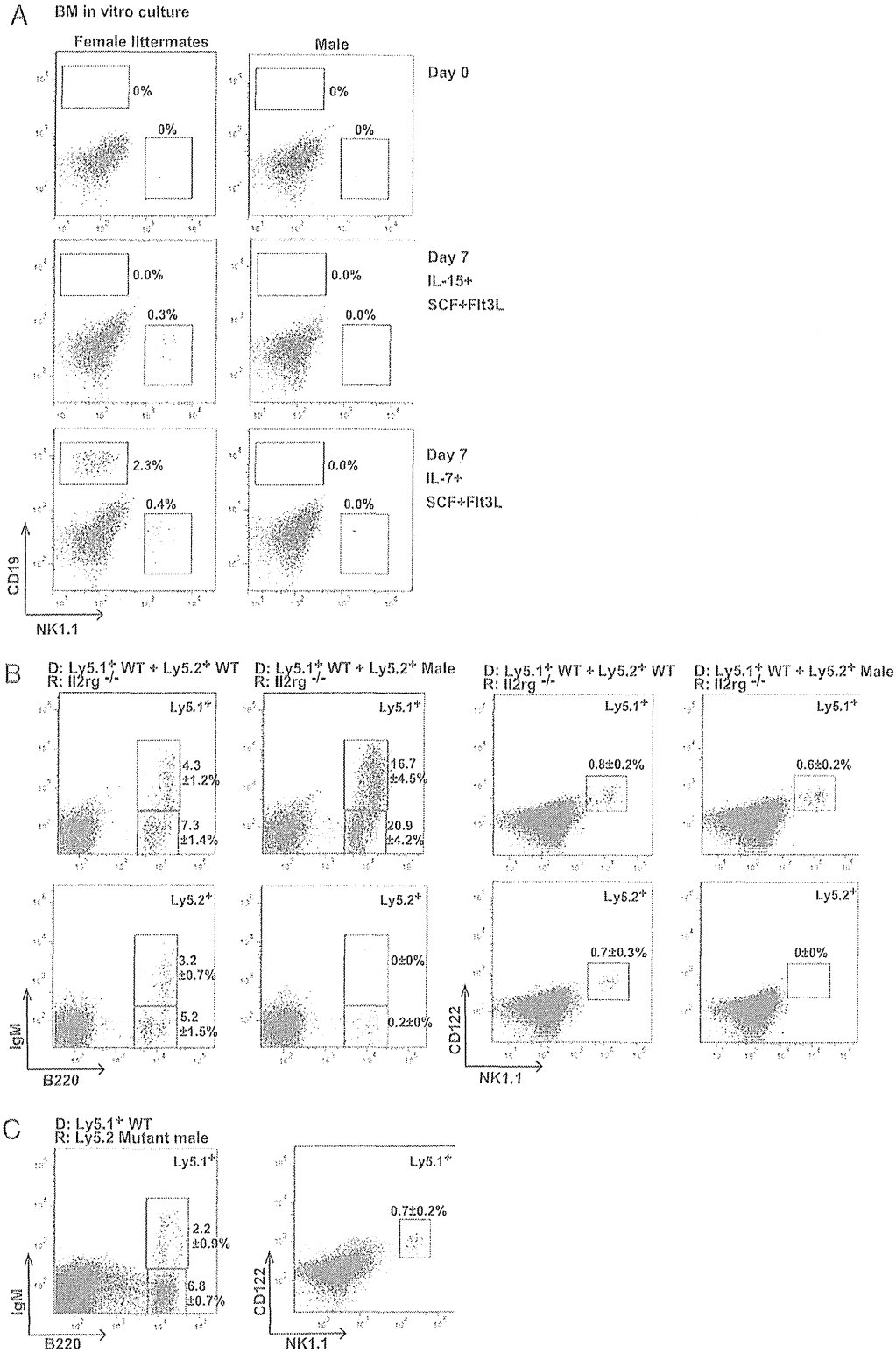

FIGURE 6. Cell-intrinsic failure of adult B cell and NK cell development. (**A**) In vitro differentiation of NK ($NK1.1^+$) and B ($CD19^+$) cells from bone marrow cells. HPCs ($B220^-$, $Thy1^-$, $DX5^-$, $Ter119^-$, $Gr\text{-}1^-$, $CD11b^-$) from the bone marrow of adult male or female littermates were cultured on OP9 stromal cells in the presence of exogenous cytokines. Numbers in plots indicate the percentages of live cells. Data are representative from two independent experiments. (**B**) B (*left panel*) and NK (*right panel*) cells generated in the bone marrow 8 wk after the reconstitution of irradiated *Il2rg*$^{-/-}$ recipients transfused with a 1:1 mixture of wild-type (Ly5.1) and wild-type (Ly5.2) or mutant male (Ly5.2) bone marrow cells. Numbers on each gate indicate the percentage relative to $Ly5.1^+$ or $Ly5.2^+$ cells. (**C**) Bone marrow cells from wild-type (Ly5.1) mice were transplanted into irradiated B cell–deficient mutant male mice (Ly5.2). B and NK cells in the bone marrow were analyzed 8 wk after reconstitution. Numbers on gates indicate the percentage relative to $Ly5.1^+$ cells. Data are from two independent experiments (n = 3 or 4 recipient mice per genotype). D, donor; R, recipient.